Diogo Lopes Soares

Licenciado em Ciências da Engenharia Electrotécnica e de Computadores

Design of multidimensional compact constellations with high power efficiency

Dissertação apresentada para obtenção do Grau de Mestre em Engenharia Electrotécnica e de Computadores, pela Universidade Nova de Lisboa, Faculdade de Ciências e Tecnologia.

Orientador: Rui Dinis, Professor Auxiliar com Agregação, FCT-UNL

Orientador: Marko Beko, Professor Auxiliar, FCT-UNL

Júri:

Presidente: Prof. Doutor Luís de Oliveira

Vogais: Prof. Doutor Rui Dinis

Prof. Doutor Marko Beko

Prof. Doutor Paulo Montezuma

FACULDADE DE CIÊNCIAS E TECNOLOGIA
UNIVERSIDADE NOVA DE LISBOA

Setembro, 2013

Design of multidimensional compact constellations with high power efficiency

” At one point in your life you either have the thing you want or the reasons why you don’t ”

Andy Roddick

Acknowledgements

Gostaria de começar por agradecer a ambos os meus coordenadores: Prof. Marko Beko e Prof. Rui Dinis, pela oportunidade de trabalhar neste tema e por todo o apoio, inspiração e disponibilidade sempre mostrada para comigo.

Para os meus pais, vai o meu maior agradecimento, pois sinto a necessidade de os destacar acima do resto: obrigado Pai e Mãe por todo o carinho, paciência, por todo o esforço e por nunca desistirem de mim. Foram sem dúvida a minha maior força ao longo destes anos.

À minha querida avó Didi, pela educação e por todo o amor que sempre me deste, obrigado. Ao meu irmão Francisco obrigado por seres o meu melhor amigo e pela amizade incondicional. À Raluca, obrigado por seres o grande apoio e conforto que eu encontro quando chego a casa.

Resta-me dizer que me sinto extremamente sortudo por chegar ao fim deste percurso e ver todas as amizades que fiz, todas as pessoas que acreditaram em mim e que sempre me empurraram para a frente. Um sincero obrigado a todos eles.

Sumário

Cada vez mais os sistemas de comunicação móveis exigem a adopção de sistemas com elevados aproveitamentos de espectro e potência. Um desenho eficaz de constelações de sinais apresenta-se como uma boa solução a este problema e pode significar um ganho energético bastante notório, o que diminuiria a energia total consumida pelos dispositivos. Os símbolos numa constelação de sinais podem ser vistos como vectores num espaço Euclidiano N-dimensional. Ao nível de uma constelação com M símbolos, a eficiência de potência pode ser melhorada procurando aumentar a distância entre símbolos para uma dada energia de bit. Contudo, no cenário dum sistema de comunicação móvel, a largura de banda apresenta-se como um factor bastante limitador.

O balanço entre a ocupação de espectro e a potência exigida permite encarar o desenho de constelações como um problema de optimização, mais concretamente como um problema de optimização não convexo Quadratically Constrained Quadratic Programming.

Considerando o facto das modulações empregues ao nível das comunicações não serem geralmente boas em termos de eficiência de potência, nomeadamente para tamanhos de constelações médio e grandes, este trabalho pretende gerar e propor novos códigos, melhores que os já existentes, focando o objectivo de optimizar a eficiência de potência para constelações de pequena e média dimensão.

Palavras Chave: Constelações multidimensionais, Eficiência de Potência, Optimização Convexa.

Abstract

More and more, mobile communication systems demand the adoption of high spectral and power efficiency systems. A good signal constellation design shows up as a good solution to this problem and may symbolize a remarkable energy gain, what would reduce the total devices' energy consumption. Considering an M symbols constellation, power efficiency can be improved by increasing the distance between symbols for a given average bit energy. Symbols belonging to a constellation can be seen as vectors in an N-dimensional space. However, in a mobile communications scenario, bandwidth emerges as a very restrictive factor.

The trade-off between spectrum occupation and power requirements enables to treat the constellations design as an optimization problem, more precisely as a non convex Quadratically Constrained Quadratic Programming problem.

Considering the fact that the modulations used in communications nowadays are not good in terms of power efficiency, particularly for medium and big sized constellations, this work intends to propose new codes better than the existent ones, aiming to optimize the power efficiency of small-to-medium sized constellations.

Keywords: multidimensional constellations, power efficiency, convex optimization.

Acronyms

ACG *Asymptotic Code Gain*

ANNN *Average Number of Nearest Neighbours*

APSK *Amplitude-Phase Shift Keying*

AWGN *Additive White Gaussian Noise*

BPSK *Binary Phase Shift Keying*

CCP *Convex Concave Procedure*

CDF *Cumulative Distribution Function*

DCP *Disciplined Convex Programs*

GD *Gradient Descent*

IB-DFE *Iterative Block Decision Feedback Equalisation*

ISI *Intersymbol Interference*

LP *Linear Programs*

M^2-QAM *M^2 Quadrature Amplitude Modulation*

NP *Non-deterministic Polynomial-time*

PAM *Pulse Amplitude Modulation*

PDF *Probability Density Function*

PSD *Power Spectral Density*

QAM *Quadrature Amplitude Modulation*

QCQP *Quadratically Constrained Quadratic Programming*

QP *Quadratic Programs*

SC-FDE *Single-Carrier Frequency-Domain-Equalization*

SDP *Semidefinite Programs*

SER *Symbol Error Rate*

SNR *Signal-to-Noise Ratio*

SOCP *Second-Order Cone Programming*

Contents

Acknowledgements iii

Abstract vii

Acronyms ix

1 Introduction 1

1.1 Motivation . . . 2
1.2 Objectives . . . 2
1.3 Structure of the dissertation . . . 3

2 Signal Spaces and Detection Theory 5

2.1 Signal Space Representations . . . 6
2.1.1 A vector Analysis . . . 6
2.1.2 Signal spaces . . . 7
2.1.3 Distances and energies . . . 9
2.1.4 Noise . . . 11
2.1.5 Optimal receptor . . . 13
2.1.6 Error probabilities . . . 15
2.1.6.1 BPSK . . . 16
2.1.6.2 Orthogonal . . . 17
2.1.6.3 Unipolar Binary . . . 18
2.1.6.4 4-PAM . . . 19
2.1.6.5 16-QAM . . . 21
2.1.6.6 N-Orthogonal . . . 23
2.1.6.7 Constellations Performance . . . 24
2.2 Modulation Techniques . . . 25
2.2.1 Multidimensional signals . . . 25
2.2.2 Biorthogonal signals . . . 25
2.2.3 Simplex signals . . . 25

3 Problem Formulation and Proposed Method **27**
3.1 Mathematical Optimization . . . 27
3.1.1 Convex Optimization Problem . . . 27
3.1.2 Non-convex Optimization Problem . . . 28
3.1.3 Non-convex QCQPs . . . 28
3.2 Problem Formulation . . . 29
3.3 Proposed Method . . . 30
3.3.1 Encountering a feasible point . . . 31
3.3.2 Normalization . . . 31
3.3.3 Linearization . . . 32
3.3.4 CVX treatment of the SOCP . . . 35
3.4 Convex Optimization software - CVX . . . 36
3.4.1 Some used commands and notions . . . 36

4 Numerical Results **39**
4.1 Complexity of the method . . . 39
4.2 CCP constellations results . . . 40
4.3 Performance results . . . 41
4.3.1 Energy cost of 2-dimensional constellations . . . 41
4.3.1.1 CCP vs Gradient Descent . . . 41
4.3.1.2 CCP vs APSK . . . 46
4.3.1.3 CCP vs QAM . . . 48
4.3.1.4 2-dimensions overall comparison . . . 49
4.3.2 Energies and gains for 3 and 4 dimension signal constellations . . . 51
4.3.2.1 3-dimensional performance comparison . . . 51
4.3.2.2 4-dimensional performance comparison . . . 52
4.3.3 Orthogonal and related signal sets performance . . . 52
4.3.4 Multidimensional K-PAM constellations performance . . . 53
4.3.5 Kissing numbers . . . 55
4.3.5.1 Comparison of kissing number constellations' values of energy vs CCP . . . 55
4.4 Performance analysis . . . 56

5 Conclusions **61**
5.1 Final Considerations . . . 61
5.2 Future Work . . . 62

Bibliography **63**

List of Figures

2.1 Conceptualized model of a digital communication system 7
2.2 Model for received signal passed through an AWGN channel 11
2.3 Bank of correlators 12
2.4 Effect of noise perturbation on location of the received signal 14
2.5 Optimal receptor 15
2.6 BPSK constellation and decision regions 16
2.7 Signal points for binary orthogonal signals 17
2.8 Signal points for binary unipolar signals 18
2.9 4-PAM signal constellation 20
2.10 16-QAM signal constellation 21

3.1 Feasible disposition for (N.M) = (2,12) 31
3.2 Normalized constelation by a $\lambda = 0.7$ factor for (N.M) = (2,12) 32

4.1 Constellation coordinates for N=5 and M=16 40
4.2 Gradient Descent constellation with M=4 42
4.3 Gradient Descent constellation with M=7 42
4.4 Gradient Descent constellation with M=8 43
4.5 Gradient Descent constellation with M=16 43
4.6 Gradient Descent constellation with M=19 44
4.7 4+12-APSK signal constellation with $\rho = 2.70$, $r_1 = 0.09014$ and $r_2 = 0.283945$ 46
4.8 4+12+16-APSK signal constellation with $\rho_1 = 2.53$, $\rho_2 = 4.3$, $r_1 = 0.046$, $r_2 = 0.125$ and $r_3 = 0.2241$ 47
4.9 16-QAM signal constellation and its derivatives 8-QAM and 7-QAM 48
4.10 36-QAM signal constellation and its derivatives 32-QAM and 19-QAM . . . 49
4.11 Comparison of CCP, GD, APSK and QAM for M=4, M=7 and M=8 50
4.12 Comparison of CCP, GD, APSK and QAM for M=16, M=19 and M=32 . . 50
4.13 Performance comparison of CCP and $(\mathrm{K}-\mathrm{PAM})^{\mathrm{N}}$ constellations for (N,M)=(4,256) and (7,128) 58
4.14 Performance comparison of CCP and $(\mathrm{K}-\mathrm{PAM})^{\mathrm{N}}$ constellations for (N,M)=(6,64) and (8,256) 58

List of Tables

2.1 Values of K for different modulations 24

4.1 Asymptotic Code Gain for CCP constellations 41
4.2 Comparison between CCP and GD for M=4 44
4.3 Comparison between CCP and GD for M=7 45
4.4 Comparison between CCP and GD for M=8 45
4.5 Comparison between CCP and GD for M=16 45
4.6 Comparison between CCP and GD for M=19 45
4.7 Comparison between CCP and APSK for M=16 47
4.8 Comparison between CCP and APSK for M=32 47
4.9 CCP and QAM energy comparisons 49
4.10 3-dimensional clusters' energy values 51
4.11 4-dimensional clusters' energy values 52
4.12 Comparison between CCP and simplex constellation for N=4 and M=4 . . 52
4.13 Comparison between CCP and simplex constellation for N=8 and M=8 . . 53
4.14 Comparison between CCP and Bi-Orthogonal Constellation for N=4 and M=8 53
4.15 Comparison between CCP and Bi-Orthogonal constellation for N=8 and M=16 53
4.16 $(K - PAM)^N$ energy values 54
4.17 CCP energy values for $(K - PAM)^N$ possible sets 54
4.18 Energy of kissing number schemes by CCP 56
4.19 ANNN for the generated constellations with **N** - number of dimensions and **M** - number of symbols 57

List of Symbols

b_i	limit of constraint $f_i(x)$
d_{ij}^2	squared distance between signal i and j
d_{min}^2	minimum squared distance
D	Euclidean distance
E_b	average bit energy
E_S	average symbol/signal energy
$\mathbf{e}_i$	basis vector
$f_0(x)$	objective function
$f_i(x)$	constraint function
K	normalized distance to $D/\sqrt{E_b}$
M	number of constellation symbols
$\mathcal{M}$	matrix of constellation vectors
m_i	transmitted symbol
$\hat{m}$	estimate symbol
N	number of constellation dimensions
N_0	Noise power spectral density

p_i	probability of transmitting symbol i
P_b	bit error probability
P_s	symbol error probability
R	ratio bits per dimensions
R_w	autocorrelation function of noise process w(t)
$\bar{s}$	mean value of vector $\mathbf{s}$
s'	origin centred vector $\mathbf{s}$
s_i	transmitted signal
T	symbol time duration
v_n	n^{th} component of vector $\mathbf{v}$
$w(t)$	additive zero-mean stationary white Gaussian noise
$x(t)$	received signal
X_j	correlator's output
$\mathcal{C}$	signal constellation
$\phi_i(t)$	i^{th} basis function
σ	standard deviation
σ_N^2	variance of channel noise

Chapter 1

Introduction

Digital communications is a wide area involving subjects from the information source until the output transducer. However, its most basic purpose involves the transmission of information under a digital form from information generative source until one or more destinations.

A great part of the transmission process is related with the transformation of the source data into some digital format in a way that information can be converted suitable to flow to the receiver through cables, fibres or through the air.

Good spectral and power efficiencies allow communications to achieve high data bit rates and to minimize the power consumption in mobile devices. It is also known that a greater spectral efficiency implies an increasing of power usage and a consequent decrease of power efficiency which is strongly undesired nowadays.

A good way to achieve a favourable trade-off between spectral and power efficiency comes from the shaping gain of a modulation. The overall gain of a transmission can be separated in two: coding gain and shaping gain. While coding gain is related with the *Signal-to-Noise Ratio* (SNR) levels between the coded system and the uncoded system, the shaping gain refers to the resulting reduction in signal constellation power [FHW98]. Shaping gain is strongly related with the modulation efficiency, namely the constellation design. For this reason the design of constellations with good power efficiency emerges as a good way to solve this problem.

1.1 Motivation

Presently, with the great increasing of communication devices, the limitations of spectra are more and more felt. As so, systems have to be planned and implemented to take the best of the actual resources. As a valid solution to the power efficiency problems of actual modulations, this work aims to obtain optimal constellations in terms of power efficiency. In this sense, it will be implemented a method that looks for the minimal energy cost schemes, improving the energy gains. Concretely, what is proposed is an optimization method that intends to minimize the transmit power for a given error rate, contrarily to the existent modulations that are not capitalizing the best of actual conditions.
The results sought are good solutions to implement in systems minimizing their energy consumption.

1.2 Objectives

The main goal of this dissertation is to find out good signal constellations that overcome the traditional modulations in what concerns to their energy cost. More precisely, this work looks for the minimum energy constellation that respects the minimum Euclidean distance between different constellation symbols greater or equal to 1.
The work is focused on small-to-medium sized constellations due to its more common use in actual systems, namely on a range of dimensions N from $2 \leq \mathrm{N} \leq 8$ and number of constellation points M where $M = 2^k$ with $k = 2, 3, 4, 5, 6, 7, 8$.
It will be presented herein a reformulation linearization-based method to find the minimum energy constellations. This practice is also known as *Convex Concave Procedure* (CCP). It turns the constellations design, originally formulated as a nonconvex *Quadratically Constrained Quadratic Programming* (QCQP) problem, which is difficult to solve, into a convex *Second-Order Cone Programming* (SOCP) problem. The SOCP problem can be solved efficiently by a convex optimization software, producing as result a new constellation with lower average symbol energy.
Finally, the idea is to call iteratively this procedure, what results in lower energy cost constellations and better power efficiencies.

1.3 Structure of the dissertation

The document is divided in 5 different chapters, as follows:

On chapter number 2, named Signal Spaces and Detection Theory, it is presented the trade-off between power efficiency and spectral efficiency in a scenario of digital communications; in section 2.1 there are introduced the representations of signals, with the essential definitions of orthogonality, symbol average energy and average probability of error for several modulations. The tour to a better understanding of signal constellations starts with a vector approach which enables the reader to percept the definition of signal spaces as well as Euclidean distances, fundamental to the formulation of the problem in chapter 3. Subsection 2.1.4 introduces the notion that a communication channel has to deal with noise and interference. It is followed by the receptor theory where detection is explained. In subsection 2.1.6 there are shown and compared the performances of: *Binary Phase Shift Keying* (BPSK), orthogonal, unipolar binary, 16-*Quadrature Amplitude Modulation* (QAM) and N-orthogonal signal constellations. The second part of the chapter introduces high power efficient constellations, namely biorthogonal and simplex constellations.

Follows chapter 3, where the design of constellations with high power efficiency is addressed as an optimization problem. In section 3.1 some mathematical optimizations like convex optimizations and the nonconvex cases are explained and distinguished. Subsection 3.2 introduces the problem formulation under the lights of convex optimization literature. It contains the clarification of the chosen values for the problem constraints and the analysis of problem convexity. Follows the core subsection 3.3 with the proposed optimization method, explained in detail, with all the steps figuring in the algorithm and a briefly explanation of each one of them. Finally, the last section of this chapter contains an introduction to the Matlab's convex optimization toolbox CVX, explaining its compatibility with the problem and the reason of its choice.

Chapter 4 is where all the results are presented. It contains the numerical results, the comparison of all the performances and the analysis of the results, with respective conclusions. First, simulations' details are clarified, such as the number of trials, the set of (N,M) pairs evaluated. It is also showed the complexity of the method in the worst

case, as well as the parameters that permit comparing the constellations. It follows the comparison of good known modulations with the proposed ones. These comparisons are first made for 2-dimensional modulations in subsection 4.3.1, where Gradient Descent, *Amplitude-Phase Shift Keying* (APSK) and QAM modulations' signal constellations are normalized and compared with the ones obtained through CCP. It follows the comparison with Sloane's proposed clusters in 3 and 4-dimensions in subsection 4.3.2. In 4.3.3 some cases of simplex and bi-orthogonal constellations are used to evaluate the performance in cases where N=M and M=2N. Finally, multidimensional *K-Pulse Amplitude Modulation* (PAM) constellations are compared with some sets (N,M), highlighting the special importance of the comparison with some 256 symbols constellations. In section 4.3.5 it is presented some theory of the kissing number and sphere packing problems, where theoretical optimal lattices, including Voronoi constellations are compared with the ones generated by the proposed method.

Finally, chapter 5 contains a briefly judgement of the method's effectiveness and the final conclusions. In subsection 5.2 are presented some ideas for possible future works taking this dissertation as reference.

Chapter 2

Signal Spaces and Detection Theory

In what respects to real systems, severe power and bandwidth constraints are encountered. This brings the urgency of adopting power and spectral efficient systems.

The choice of the best signal constellation is not an easy task, however, setting a value for its average signal energy, here designated by E_S, an optimum signal constellation is the one that achieves a specified error probability with the lowest value of E_S.

It has been proved analytically that the error probability can be made as small as desired by increasing the number of symbols in a constellation. However, what happens is that more than the increasing of receiver complexity, a bigger occupation of bandwidth is required, which leads to a reduction of spectral efficiency [CC75].

This brings the need to highlight that a careful trade-off between power efficiency and spectral efficiency is required to choose the most suitable constellation for a certain system, especially in the case of multidimensional constellations, where the increase of the number of dimensions implies loss of spectral efficiency but at the same time it allows an improvement of power efficiency.

In this chapter there will be exposed some important concepts essential to judge power and spectral effectiveness of the signal sets, as well as their energy costs and gains, fundamental to a good understanding of the developed work.

2.1 Signal Space Representations

2.1.1 A vector Analysis

Vector spaces are the subject of linear algebra and are characterized by their dimension, which specifies the number of independent directions in the space. A vector space may be characterized with additional structures, such as norm and inner product. These spaces arise naturally in mathematical analysis and abundantly in the form of infinite-dimensional function spaces whose vectors are functions.

A vector $\mathbf{v}$ in an n-dimensional space is characterized by its n components $[v_1 v_2 \cdots v_n]$. It may also be represented as a linear combination of *basis vectors* $\mathbf{e}_i$, $1 \leq i \leq n$, as showed in equation

$$\mathbf{v} = \sum_{i=1}^{n} v_i \mathbf{e}_i \tag{2.1}$$

where, by definition, basis vectors have unitary length. The vector component v_i is the projection of the vector $\mathbf{v}$ onto the unit vector $\mathbf{e}_i$. Thus vector $\mathbf{v}_i$ becomes

$$\mathbf{v}_i = \sum_{j=1}^{n} v_{ij} \mathbf{e}_j = (v_{i1}, \cdots v_{in}) \tag{2.2}$$

One of the basic properties of vectors is the inner product, represented by a dot and denoted $\mathbf{v}_1 \cdot \mathbf{v}_2$. It returns a scalar value and its basic form is defined as

$$\mathbf{v}_1.\mathbf{v}_2 = \|\mathbf{v}_1\| \|\mathbf{v}_2\| \cos\theta \tag{2.3}$$

where θ is the measure of the angle between $\mathbf{v}_1$ and $\mathbf{v}_2$.

Applied to two n-dimensional vectors $\mathbf{v}_1 = [v_{11} v_{12} \cdots v_{1n}]$ and $\mathbf{v}_2 = [v_{21} v_{22} \cdots v_{2n}]$, inner product is defined as

$$\mathbf{v}_1.\mathbf{v}_2 = \sum_{i=1}^{n} v_{1i} v_{2i} \tag{2.4}$$

This operation is a simple way to determine whether the vectors are orthogonal or not.

Generally, a set of m vectors $\mathbf{v}_i$, $1 \leq i \leq m$, are orthogonal if

$$\mathbf{v}_i.\mathbf{v}_j = 0 \tag{2.5}$$

for all $1 \leq i, j \leq m$ and $i \neq j$.

Other vectors' basic property is the norm, also called length, denoted $||\mathbf{v}||$ and defined as

$$||\mathbf{v}|| = \sqrt{(\mathbf{v}.\mathbf{v})} \tag{2.6}$$

The squared-length of a vector is defined to be the inner product of the vector $\mathbf{v}$ with itself, as it can be checked on 2.6 by squaring both sides of the equation. It can also be written as the sum of the squared components of the vector

$$||\mathbf{v}||^2 = \sum_{i=1}^{n} v_i^2 \tag{2.7}$$

These vectors' properties of 2.5 and 2.6, may be used to verify if a set of vectors is *orthonormal*. Clearly, a set of vectors is said to be *orthonormal* if the vectors besides being orthogonal also have length 1.

2.1.2 Signal spaces

In a digital communication system, like the one in figure 2.1

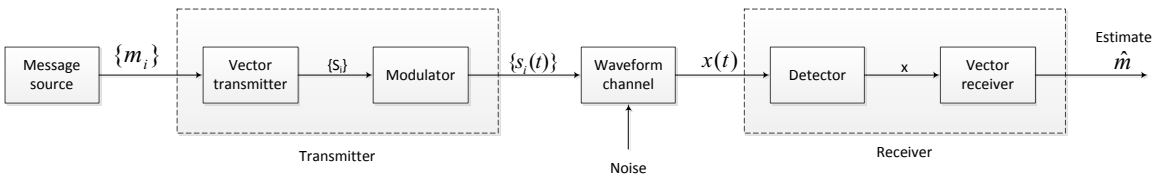

Figure 2.1: Conceptualized model of a digital communication system

the output of the message source is given to a vector transmitter every T seconds. The vector transmitter produces then a vector of real numbers. In the case of an output

message $m = m_i$, the vector transmitter output takes the value

$$\mathbf{s}_i = \begin{bmatrix} s_{i1} \\ s_{i2} \\ \vdots \\ s_{iN} \end{bmatrix} \quad i = 1, 2, \ldots, M \tag{2.8}$$

This vector $\mathbf{s}_i$ is called the signal vector and it determines the signal $s_i(t)$ generated by the modulator. This is, receiving $\mathbf{s}_i$ as input, the modulator constructs a distinct signal $s_i(t)$ of duration T seconds with the information from the vector.

Signal $s_i(t)$ is necessarily of finite energy 2.9

$$E_i = \int_0^T s_i^2(t)\ \mathrm{dt} \tag{2.9}$$

As it can be seen, signals have characteristics resembling vectors. Thus, it is possible to develop a parallel representation for a set of signal waveforms [Pro01].

The inner product of two general real-valued signals $s_1(t)$ and $s_2(t)$ is denoted $\langle s_1(t)s_2(t)\rangle$ and it is defined as

$$\langle s_1(t), s_2(t)\rangle = \int_{-\infty}^{+\infty} s_1(t)s_2(t)\,\mathrm{d}t \tag{2.10}$$

Similarly to vector's properties, signals $s_1(t)$ and $s_2(t)$ are orthogonal if their inner product is zero.

However, the norm, assumes a much more important role in what concerns signals. Despite it is defined in the same way as the vectorial norm,

$$||s(t)|| = \sqrt{\langle s(t), s(t)\rangle} \tag{2.11}$$

when considering $s(t)$ a deterministic real-valued signal with finite energy, its squared norm represents the energy of the signal, $\mathrm{E_S}$.

$$E_S = ||s(t)||^2 = \int_0^T s(t)^2\,\mathrm{d}t \tag{2.12}$$

Again regarding to vector analysis, a set of orthonormal basis functions $\phi_j(t)$, $j = 1, 2, \ldots, N$ verifies

$$\int_{-\infty}^{+\infty} \phi_i(t)\phi_j(t)\,\mathrm{d}t = \begin{cases} 0, & i \neq j \\ 1, & i = j \end{cases} \tag{2.13}$$

Thus, signals may be expressed as function of orthonormal basis functions $\phi_j(t)$ like in expression (2.14).

$$s_i(t) = \sum_{j=1}^{N} s_{ij}\phi_j(t) \tag{2.14}$$

where s_i is a point in the N-dimensional Euclidean space with coordinates $[s_{i1}, s_{i2}, \ldots, s_{iN}]$. To this N-dimensional Euclidean space is given the name of signal space.

For what matters, a group of these signals may constitute a signal constellation $\mathcal{C}$. The energy of the i^{th} signal is simply the square of the Euclidean distance from the origin to the point in the N-dimensional space. Thus, any signal can be represented geometrically as a point in the signal space spanned by the orthonormal functions $\phi_j(t)$.

2.1.3 Distances and energies

There is a close relationship between the energy content of a signal and its vectorial representation. As it was shown in (2.12) the energy of a signal $s_i(t)$ of duration T is $E_S = \int_0^T s_i^2(t)\ \mathrm{dt}$. In the same manner, the energy of the signal $s_i(t)$ is equal to the squared-length of the signal vector $\mathbf{s}_i$ representing it, by applying the vectorial expression (2.7).

$$E_S = \sum_{j=1}^{N} s_{ij}^2 \tag{2.15}$$

In the case of a pair of signals $s_i(t)$ and $s_k(t)$ whose correspondent signal vectors are $\mathbf{s}_i$ and $\mathbf{s}_k$, the distance between both signals is equal to the distance between both signal vectors $\mathbf{s}_i$ and $\mathbf{s}_k$ in the Euclidean space. Thus,

$$dist(\mathbf{s}_i, \mathbf{s}_k) = \|\mathbf{s}_i - \mathbf{s}_k\| = \sum_{j=1}^{N}(s_{ij} - s_{kj}) \tag{2.16}$$

Squaring both sides of (2.16), results the expression

$$\|\mathbf{s}_i - \mathbf{s}_k\|^2 = \sum_{j=1}^{N} (s_{ij} - s_{kj})^2 \tag{2.17}$$

where an interesting development is about to appear.

Looking at the properties of the vectorial norm and to the development of the square of a difference $(a-b)^2 = a^2 + b^2 - 2ab$, the squared-distance between signals (2.17) can be written as

$$dist^2(s_i(t), s_k(t)) = \sum_{j=1}^{N} s_{ij}^2 + \sum_{j=1}^{N} s_{kj}^2 - 2\langle s_i(t), s_k(t)\rangle \tag{2.18}$$

which is the sum of both signals energies minus the inner product between them.

$$E_i + E_k - 2\langle s_i(t), s_k(t)\rangle \tag{2.19}$$

In the special case where both signals are orthogonal, it was already seen that the inner product of the two signals is zero, which takes the expression (2.18) to assume the following form

$$dist^2(s_i(t), s_k(t)) = E_i + E_k \tag{2.20}$$

In fact, this distance is called Euclidean distance, once it respects to Euclidean space.

Many of energy references in formulas and expressions are showed in function of $\mathrm{E_b}$, average bit energy. The relation between $\mathrm{E_b}$ and $\mathrm{E_S}$ is given by

$$E_b = \frac{E_S}{number\,of\,bits\,per\,symbol} \tag{2.21}$$

The number of bits per symbol can be obtained computing $log_2 M$, where M is the number of symbols in a signal constellation. In irregular constellations, this is, that not follow traditional constellation schemes, the number of closer symbols has to be calculated for each of the constellation symbols. Two symbols $\mathbf{x}_i$ and $\mathbf{x}_j$ are considered neighbours if $1 \leq ||\mathbf{x}_i - \mathbf{x}_j|| \leq 1 + \epsilon$, where ϵ is a positive small constant used as threshold.

2.1.4 Noise

To the receiver block of figure 2.1 arrives the digital information sent by the transmitter through the transmission channel. The transmitter sends the information using M signal waveforms $s_i(t)$, $i = 1, 2, \ldots, M$. Each signal is transmitted within the symbol interval of duration T.

The channel however, corrupts the signal by adding white Gaussian noise, as seen in figure 2.2.

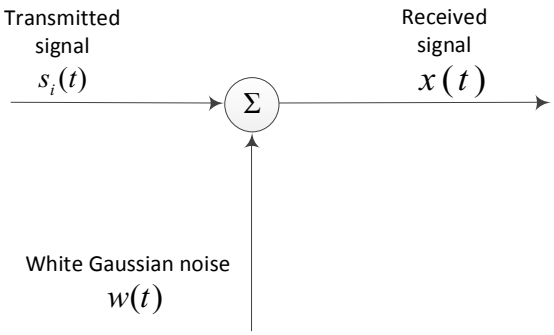

Figure 2.2: Model for received signal passed through an AWGN channel

Thus, the received signal may be expressed as

$$x(t) = s_i(t) + w(t)\,, \quad 0 \leq t \leq T\,, \tag{2.22}$$

where $w(t)$ denotes a sample function of additive white Gaussian noise characterized by zero mean and power spectral density $N_0/2$.

The scheme of figure 2.3 is composed by a set of N product-integrators, also called correlators sharing a common input: the received signal given by (2.22). Each correlator has its own $\phi_j(t)\,,\ 1 \leq j \leq N$ basis function. This scheme is used as the first stage of the receiver block showed in figure 2.1.

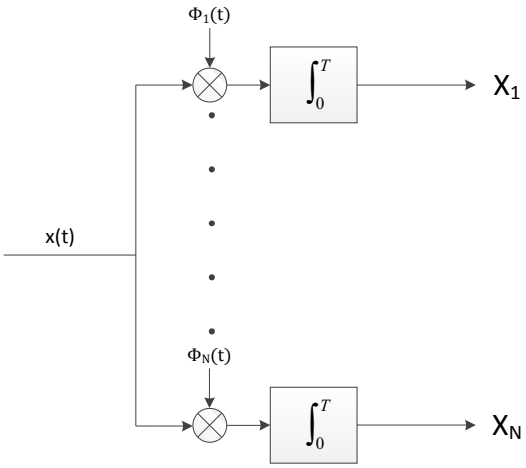

Figure 2.3: Bank of correlators

Consequently, the output of each correlator is a random variable X_j given by

$$\begin{aligned} X_j &= \int_0^T X(t)\phi_j(t)\ \mathrm{dt} \\ &= s_{ij} + W_j\,,\ \ j = 1, 2, \ldots, N \end{aligned} \tag{2.23}$$

In (2.23), the first component, s_{ij}, is a deterministic quantity contributed by the transmitted signal $s_i(t)$. Although, the second component, W_j, is a random variable that arises caused by the presence of noise in the transmission channel. It is defined as

$$W_j = \int_0^T W(t)\phi_j(t)\ \mathrm{dt}. \tag{2.24}$$

Due to the noise's nature, the received signal $x(t)$ has a Gaussian distribution, what implies that the correlator's output is also a Gaussian random variable. Hence, X_j is characterized completely by its mean value and variance.

The mean value can be discovered starting by the fact that the noise process $w(t)$ has zero mean. Which implies that the random variable W_j obtained from (2.24) has zero mean too. Thus, the mean value of the j^{th} correlator output X_j only depends on s_{ij}.

To find the variance of X_j, note that

$$\begin{aligned} \sigma_{X_j}^2 &= \mathrm{Var}[X_j] \\ &= E[W_j^2] \end{aligned} \tag{2.25}$$

Using (2.24) in (2.25), results

$$\begin{aligned} \sigma_{X_j}^2 &= E\left[\int_0^T \int_0^T \phi_j(t)\phi_j(u)W(t)W(u)\,\mathrm{dtdu}\right] \\ &= \int_0^T \int_0^T \phi_j(t)\phi_j(u)R_W(t,u)\,\mathrm{dt\,du} \end{aligned} \tag{2.26}$$

where $R_W(t,u)$ is the autocorrelation function of noise process w(t).

As the noise is stationary, R_W depends only on the time difference $t-u$. Furthermore, the noise is also white, having *Power Spectral Density* (PSD) equal to $N_0/2$. Hence, R_W can be expressed as

$$R_W(t,u) = N_0/2\delta(t-u) \tag{2.27}$$

and consequently $\sigma_{X_j}^2$ comes

$$\begin{aligned} \sigma_{X_j}^2 &= \frac{N_0}{2}\int_0^T \phi_j(t)\phi_j(u)\delta(t-u)\,\mathrm{dt\,du} \\ &= \frac{N_0}{2}\int_0^T \phi_j^2(t)\,\mathrm{dt} \\ &= \frac{N_0}{2} \end{aligned} \tag{2.28}$$

where $\phi_j(t)$ is an orthonormal basis.

This result shows that all correlator outputs have a variance equal to the PSD $N_0/2$ of the additive noise $w(t)$.

2.1.5 Optimal receptor

When the received signal $x(t)$ is applied to the bank of correlators depicted in figure 2.3, the correlators outputs define a new vector $\mathbf{x}$, called received vector. This received vector differs from the signal vector $\mathbf{s}_i$ because of the inclusion of the noise vector $\mathbf{w}$.

In figure 2.4 is shown the representation of the received signal, based on the received vector $\mathbf{x}$, built by the sum of the noise vector $\mathbf{w}$ with the signal vector, $\mathbf{s}_i$.

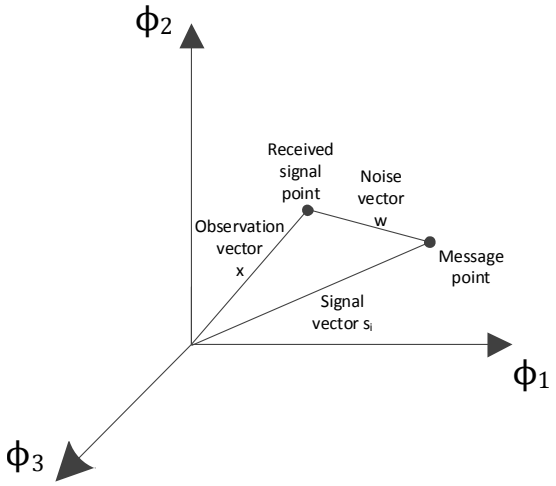

Figure 2.4: Effect of noise perturbation on location of the received signal

Arriving to this point, a mapping process from $\mathbf{x}$ has to be performed to an estimate $\hat{m}$ of the transmitted symbol, m_i, in a way that must minimize the average probability of symbol error in the decision. The average probability of symbol error in the decision, denoted P_S is

$$\begin{aligned} P_S(m_i, \mathbf{x}) &= P(m_i \text{ not sent}|\mathbf{x}) \\ &= 1 - P(m_i \text{ sent}|\mathbf{x}) \end{aligned} \tag{2.29}$$

A good detection process settles in the minimization of the distance between all the possible transmitted signal vectors [Hay88], $\mathbf{s}_i$ and the respective received vector $\mathbf{x}$

$$\begin{aligned} \min_{\mathbf{s}_i} d^2(\mathbf{s}_i, \mathbf{x}) &= \min_{\mathbf{s}_i} \|\mathbf{s}_i - \mathbf{x}\|^2 \\ &= \min_{\mathbf{s}_i} (E_i + E_x - 2\langle \mathbf{s}_i, \mathbf{x} \rangle) \end{aligned} \tag{2.30}$$

However, the expression can be simplified, dividing by two and ignoring the average bit energy of the received vector, E_x, once it is independent from the transmitted signal. Hence, (2.30) may be written as

$$\max_{\mathbf{s}_i} (\langle \mathbf{s}_i, \mathbf{x} \rangle - \frac{E_i}{2}) \tag{2.31}$$

where

$$\langle \mathbf{s}_i, \mathbf{x} \rangle = \int_0^T [s_i(t) + w(t)]\, s_i(t)\ \mathrm{dt} \tag{2.32}$$

and

$$E_i = \|s_i\|^2 = \int_0^T s_i^2(t)\ \mathrm{dt}. \tag{2.33}$$

Thus, the optimal receptor can take the form presented in figure 2.5

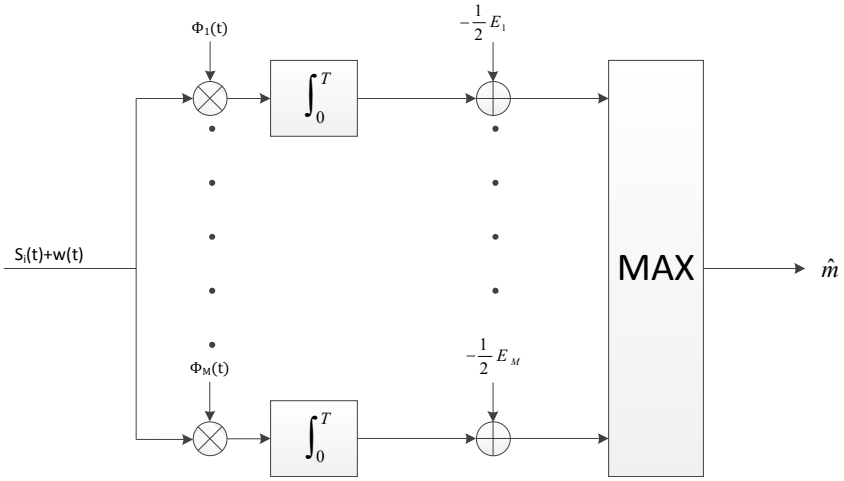

Figure 2.5: Optimal receptor

2.1.6 Error probabilities

The model of a Gaussian distribution plays a really important role in what concerns the detection theory. As so, it is imperative to understand some concepts.

The *Probability Density Function* (PDF) of a Gaussian distributed random variable x is

$$\mathrm{PDF}(x) = \frac{1}{\sqrt{2\pi}\sigma} e^{-(x-m_x)/2\sigma^2} \tag{2.34}$$

and the *Cumulative Distribution Function* (CDF) of a Gaussian distributed random variable x is defined as

$$\begin{aligned} F(x) &= \int_{-\infty}^{x} p(u)\ \mathrm{du} \\ &= \frac{1}{2}\frac{1}{\sqrt{\pi}} \int_{-\infty}^{(x-\bar{x})/\sqrt{2}\sigma} e^{-t^2} \\ &= \frac{1}{2} + \frac{1}{2}\mathrm{erf}\left(\frac{x-\bar{x}}{\sqrt{2}\sigma}\right) \end{aligned} \tag{2.35}$$

where $\mathrm{erf}(x)$ denotes the error function, defined as

$$\mathrm{erf}(x) = \frac{1}{\sqrt{\pi}} \int_x^{\infty} e^{-t^2} \tag{2.36}$$

For $x > \bar{x}$ the complementary error function $\mathrm{erfc}(x) = \frac{2}{\sqrt{\pi}} \int_x^{\infty} e^{-t^2}$ is proportional to the area under the tail of a Gaussian PDF [Pro01]. Thus, it was adopted a function to denote the area under the tail of a Gaussian PDF, denoted $Q(x)$ and defined as

$$Q(x) = \frac{1}{\sqrt{2\pi}} \int_x^{\infty} e^{-t^2/2} \, \mathrm{dt} \qquad x \geq 0 \tag{2.37}$$

2.1.6.1 BPSK

For the antipodal binary constellation represented in figure 2.6, the set of signal vectors represented are $\mathbf{s}_1 = -\frac{D}{2}$ and $\mathbf{s}_2 = \frac{D}{2}$.

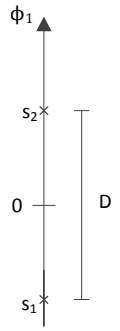

Figure 2.6: BPSK constellation and decision regions

Therefore, the energy of signal $s_1(t)$ can be written as $E_1 = \left(\frac{D}{2}\right)^2 = \frac{D^2}{4}$. The same is valid for $s_2(t)$, which results in average energy per bit

$$E_b = \frac{D^2}{4} \tag{2.38}$$

for BPSK constellations.

The decision process relies on the choice of the transmitted signal, comparing the received signal vector $\mathbf{x}$, with the threshold zero. In case $\mathbf{x} < 0$, it is assumed that signal $s_1(t)$ was transmitted, in case $\mathbf{x} > 0$ the decision taken is that it was transmitted the signal $s_2(t)$. Assuming that $s_1(t)$ was transmitted, the probability of error is the probability that $\mathbf{x} >$

$D/2$, this is,

$$P_b = P\left(\mathbf{x} > \frac{D}{2}\right) \tag{2.39}$$

which is equivalent to

$$Q\left(\frac{D/2}{\sigma_w}\right) = Q\left(\sqrt{\frac{D^2/2}{N_0/2}}\right) = Q\left(\sqrt{\frac{2E_b}{N_0}}\right) \tag{2.40}$$

Since signals $s_1(t)$ and $s_2(t)$ are equally likely to be transmitted, the average probability of error is

$$\begin{aligned} P_b &= \frac{1}{2}P(e|s_1) + \frac{1}{2}P(e|s_2) \\ &= Q\left(\sqrt{\frac{2E_b}{N_0}}\right) \end{aligned} \tag{2.41}$$

As it can be verified in relation (2.41), the probability of error only depends on the ratio E_b/N_0. This ratio is called signal-to-noise ratio per bit.

2.1.6.2 Orthogonal

The type of signal constellation called orthogonal is shown in figure 2.7

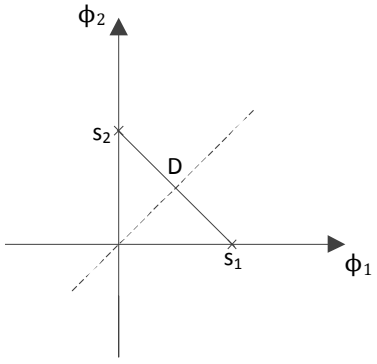

Figure 2.7: Signal points for binary orthogonal signals

Here, signals $s_1(t)$ and $s_2(t)$ are orthogonal and signal vectors $\mathbf{s}_1$ and $\mathbf{s}_2$ are two-dimensional, being defined as $\mathbf{s}_1 = \begin{bmatrix}\sqrt{E_b} & 0\end{bmatrix}$ and $\mathbf{s}_2 = \begin{bmatrix}0 & \sqrt{E_b}\end{bmatrix}$, where $\sqrt{E_b}$ denotes the energy of each of the waveforms. Remark that the distance between both signals is $D = \sqrt{2E_b}$ Assuming that signal $s_1(t)$ was transmitted, the received signal vector from the correlator is $\mathbf{x} = \begin{bmatrix}\sqrt{E_b} + \mathbf{w}_1 & \mathbf{w}_2\end{bmatrix}$.

The probability of error is the probability that the correlation C between the received signal vector and the transmitted signal $C(\mathbf{x}, \mathbf{s}_1)$ is smaller than the correlation between the received signal vector and the not transmitted signal $C(\mathbf{x}, \mathbf{s}_2)$. It can be expressed as

$$P(e|\mathbf{s}_1) = P\left[C(\mathbf{x}, \mathbf{s}_2) > C(\mathbf{x}, \mathbf{s}_1)\right] = P\left[\mathbf{w}_2 - \mathbf{w}_1 > \sqrt{E_b}\right] \tag{2.42}$$

and $P\left(\mathbf{w}_2 - \mathbf{w}_1 > \sqrt{E_b}\right)$ returns

$$P\left(\mathbf{w}_2 - \mathbf{w}_1 > \sqrt{E_b}\right) = Q\left(\sqrt{\frac{E_b}{N_0}}\right) \tag{2.43}$$

once $\mathbf{w}_2 - \mathbf{w}_1$ is zero mean Gaussian with variance N_0.

Due to the symmetry of the constellation, the same error probability is obtained when $s_2(t)$ is assumed to be transmitted. Consequently, the average error probability for binary orthogonal signals is

$$P_b = Q\left(\sqrt{\frac{E_b}{N_0}}\right) \tag{2.44}$$

2.1.6.3 Unipolar Binary

Considering the unipolar constellation represented in figure 2.8, the set of signal vectors represented are $\mathbf{s}_1 = \sqrt{E_b}$ and $\mathbf{s}_2 = 0$.

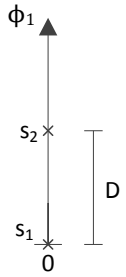

Figure 2.8: Signal points for binary unipolar signals

Like in section 2.1.6.1, the received signal vector is

$$\mathbf{x} = \mathbf{s}_i + \mathbf{w} \tag{2.45}$$

The only difference between the two modulations at this point is that the decision of what was the transmitted signal compares x with the threshold $D/2$.

Assuming that the signal $s_1(t)$ was transmitted, the probability of error is the probability of $\mathbf{x} < \frac{D}{2}$, this is

$$P_b = P\left(\frac{D/2}{\sigma_n}\right) = P\left(\sqrt{\frac{D^2/2}{N_0}}\right) \tag{2.46}$$

In order to write the probability of error in terms of E_b/N_0, E_b has to be calculated. So:

$$E_1 = \sum_{j=1}^{N} s_{ij}^2 = D^2 \tag{2.47}$$

$$E_2 = 0 \tag{2.48}$$

Assuming that both signals are equal likely to be transmitted, the average error probability per bit is

$$Eb = \frac{1}{2}E_1 + \frac{1}{2}E_2 = \frac{D^2}{2} \tag{2.49}$$

Substituting E_b value in (2.46), it becomes

$$P_e = P\left(\sqrt{\frac{E_b}{N_0}}\right) \tag{2.50}$$

This result shows that the performance of a unipolar binary constellation is the same as an orthogonal signal constellation.

2.1.6.4 4-PAM

Figure 2.9 shows a 4-PAM signal constellation, where signals $s_1(t)$, $s_2(t)$, $s_3(t)$ and $s_4(t)$ are represented by the signal vectors

$$\mathbf{s}_1 = \left(\frac{3}{2}D\right) \tag{2.51}$$

$$\mathbf{s}_2 = \left(\frac{1}{2}D\right) \tag{2.52}$$

$$\mathbf{s}_3 = \left(-\frac{1}{2}D\right) \tag{2.53}$$

$$\mathbf{s}_4 = \left(-\frac{3}{2}D\right) \tag{2.54}$$

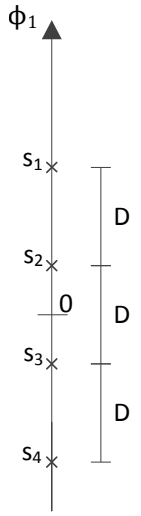

Figure 2.9: 4-PAM signal constellation

Error probabilities are calculated considering the number of neighbours that each symbol has. In case of M-PAM constellations there are two types: the middle symbols ($\mathbf{s}_2$ and $\mathbf{s}_3$) and the edge symbols ($\mathbf{s}_1$ and $\mathbf{s}_4$).

Assuming that signal $s_1(t)$ was transmitted, the P_s is just the probability of the received vector to be in the detection range of $s_2(t)$. This is:

$$P_{S1} = Q\left(\frac{D/2}{\sigma_w}\right) \tag{2.55}$$

The same is verified when transmitting $s_4(t)$.

In case of transmitting $s_2(t)$, errors can occur if the received vector falls either in the detection range of $s_1(t)$ or $s_3(t)$, doubling the error probability. This implies multiplying the previous error probability (2.55) by a factor 2, which results

$$P_{S2} = 2Q\left(\frac{D/2}{\sigma_w}\right) \tag{2.56}$$

$s_3(t)$ verifies the same error probability.

In this signal constellation, the average energy per bit is

$$E_b = \frac{E_1 + E_2 + E_3 + E_4}{4} \tag{2.57}$$

while the signal energies are

$$E_1 = \left(\frac{9}{4}D^2\right) = E_4 \tag{2.58}$$

$$E_2 = \left(\frac{1}{4}D^2\right) = E_3 \tag{2.59}$$

which returns an average energy per bit $E_b = \frac{10}{8}D^2 = \frac{5}{4}D^2$.

In case of 4-PAM, expression $log_2 M$ returns 2, meaning that each symbol codifies 2 bits. Thus, P_b results

$$P_b = \frac{P_s}{2} \tag{2.60}$$

where

$$P_S = \frac{P_{S1} + P_{S2} + P_{S3} + P_{S4}}{4} = \frac{3}{2}Q\left(\frac{D/2}{\sigma_w}\right) \tag{2.61}$$

Hence, (2.60) results

$$P_b = \frac{3}{4}Q\left(\frac{D/2}{\sigma_w}\right) = \frac{3}{4}Q\left(\sqrt{\frac{D^2/2}{N_0}}\right) = \frac{3}{4}Q\left(\sqrt{\frac{4}{5}\frac{E_b}{N_0}}\right) \tag{2.62}$$

2.1.6.5 16-QAM

Here, it will be explained the particular case of 16-QAM, however the generalization for $M^2 - QAM$ constellations will be also evaluated.

A regular 16-QAM constellation is presented in figure 2.10. The constellation is assumed to have Gray mapping.

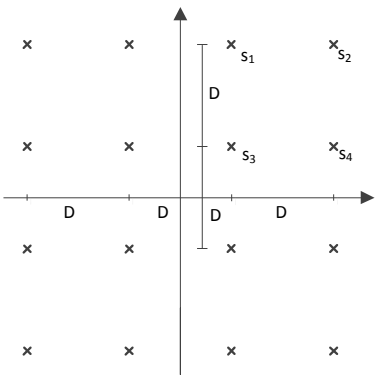

Figure 2.10: 16-QAM signal constellation

Looking at the first quadrant, there are the representations of signal vectors $\mathbf{s}_1$, $\mathbf{s}_2$, $\mathbf{s}_3$ and $\mathbf{s}_4$ with respective coordinates in the 2-dimensional Euclidean space and signal energies:

$$\mathbf{s}_1 = \left(\frac{1}{2}D,\ \frac{3}{2}D\right) \qquad E_1 = \left(\frac{1}{2}D\right)^2 + \left(\frac{3}{2}D\right)^2 = \frac{5}{2}D^2 \tag{2.63}$$

$$\mathbf{s}_2 = \left(\frac{3}{2}D,\ \frac{3}{2}D\right) \qquad E_2 = \left(\frac{3}{2}D\right)^2 + \left(\frac{3}{2}D\right)^2 = \frac{9}{2}D^2 \tag{2.64}$$

$$\mathbf{s}_3 = \left(\frac{1}{2}D,\ \frac{1}{2}D\right) \qquad E_3 = \left(\frac{1}{2}D\right)^2 + \left(\frac{1}{2}D\right)^2 = \frac{1}{2}D^2 \tag{2.65}$$

$$\mathbf{s}_4 = \left(\frac{3}{2}D,\ \frac{1}{2}D\right) \qquad E_4 = \left(\frac{3}{2}D\right)^2 + \left(\frac{1}{2}D\right)^2 = \frac{5}{2}D^2 \tag{2.66}$$

From these values, the average energy per symbol in the first quadrant is easily obtained

$$E_S = \frac{E_1 + E_2 + E_3 + E_4}{4} = \frac{5}{2}D^2 \tag{2.67}$$

As each symbol codifies $log_2(16) = 4$ bits, the average energy per bit is obtained by simply dividing E_S per 4

$$E_b = \frac{E_S}{4} = \frac{5}{8}D^2 \tag{2.68}$$

Note that, when transmitting signal $s_1(t)$ for instance, more than one error can occur, which is provoked by the fact that the received signal vector can be positioned in the detection area of any of the 3 neighbour signals. This multiplies by a factor 3 the probability of occurring an error in the detection.

All signals are separated from their neighbours by the same distance D, which resembling to previous subsections, the probability of error considering just one neighbour is

$$P_e = Q\left(\frac{D/2}{\sigma_w}\right) = Q\left(\sqrt{\frac{D^2/4}{N_0/2}}\right) = Q\left(\sqrt{\frac{4}{5}\frac{E_b}{N_0}}\right) \tag{2.69}$$

Although, for $s_1(t)$ the error can occur for 3 different signals, which implies

$$P_{S_1} = 3Q\left(\sqrt{\frac{4}{5}\frac{E_b}{N_0}}\right) \tag{2.70}$$

For the rest of the signals (of the first quadrant), their probabilities of error are

$$P_{S_2} = 2Q\left(\sqrt{\frac{4}{5}\frac{E_b}{N_0}}\right)$$

$$P_{S_3} = 4Q\left(\sqrt{\frac{4}{5}\frac{E_b}{N_0}}\right)$$

$$P_{S_4} = 3Q\left(\sqrt{\frac{4}{5}\frac{E_b}{N_0}}\right)$$

This allows the calculation of the average probability of error per symbol

$$P_S = \frac{P_{S_1} + P_{S_2} + P_{S_3} + P_{S_4}}{4} = 3Q\left(\sqrt{\frac{4}{5}\frac{E_b}{N_0}}\right) \tag{2.71}$$

Consequently, P_b is

$$P_b = \frac{3}{4}Q\left(\sqrt{\frac{4}{5}\frac{E_b}{N_0}}\right) \tag{2.72}$$

2.1.6.6 N-Orthogonal

In the case of N orthogonal signals $s_1(t), s_2(t), \ldots, s_N(t)$, each signal vector is represented as

$$\mathbf{s}_1 = (\alpha, 0, 0, \ldots, 0)$$

$$\mathbf{s}_2 = (0, \alpha, 0, \ldots, 0)$$

$$\mathbf{s}_N = (0, 0, 0, \ldots, \alpha)$$

and the respective signal energies are

$$E_S = \alpha^2 \tag{2.73}$$

with

$$E_b = \frac{E_S}{log_2(M)} \tag{2.74}$$

where M is the number of signals in the constellation.

The distance between two orthogonal signals is

$$D^2 = \|\mathbf{s}_1 - \mathbf{s}_2\|^2 = E_1 + E_2 = 2\alpha^2 \tag{2.75}$$

as showed in expression 2.20.

Hence, the probability of error for a N-orthogonal constellation results

$$P_b = Q\left(\frac{D/2}{\sigma_w}\right) = Q\left(\sqrt{\frac{D^2/2}{N_0}}\right) = Q\left(\sqrt{log_2(M)\frac{E_b}{N_0}}\right) \tag{2.76}$$

2.1.6.7 Constellations Performance

In every error probability described along subsections 2.1.6.1 to 2.1.6.6, a factor $K = \frac{D^2}{E_b}$ can be verified. This factor defines the necessary energy to obtain a certain error probability. Thus, best performance constellations are those which verify the smallest factor K.

For the referred schemes, values of K are:

Constellation Type	**K**
Antipodal	4
Orthogonal	2
Unipolar	2
4-PAM	$\frac{4}{5}$
16-QAM	$\frac{4}{5}$
N-orthogonal	$2log_2(M)$

Table 2.1: Values of K for different modulations

For example, comparing result 2.41 with 2.44, it is verified that orthogonal signals require twice the energy to achieve the same error probability as antipodal signals. Since

$10log_{10}2 = 3$dB, it leads to the conclusion that orthogonal signals are 3dB less efficient than antipodal signals.

This difference between performances is caused by the distance between the signal points in the constellations, which is $D^2 = 2E_b$ in the case of orthogonal signals and $D^2 = 4E_b$ for antipodal signals.

2.2 Modulation Techniques

2.2.1 Multidimensional signals

When it is desired to construct signal waveforms corresponding to higher-dimensional vectors, it is possible to use either the time domain, the frequency domain or even both in order to increase the number of dimensions.

Dealing with an N-dimensional signal constellation, for any N, a time interval of length $T_1 = NT$ can be divided into N subintervals of length $T = T_1/N$. In each subinterval of length T, can be used binary PAM (one-dimensional) to transmit an element of the N-dimensional signal vector. Thus, the N time slots are used to transmit a N-dimensional signal.

2.2.2 Biorthogonal signals

Considering M signal waveforms $s_m(t)$, or the vector representation $\mathbf{s}_m$, with equal probability of being transmitted. A signal set is said to be orthogonal if it is true that all M signals besides being orthogonal also have equal average energy E_S values.

A set of M biorthogonal signals can be constructed from $\frac{1}{2}$M orthogonal signals simply by adding the negative parts of each orthogonal signal. Hence, for the construction of a set of M biorthogonal signals it is required N= $\frac{1}{2}$M dimensions.

Regarding the latter situation the minimum Euclidean distance between signals is $D = \sqrt{2}E_S$.

2.2.3 Simplex signals

Suppose having a set of M orthogonal waveforms $s_m(t)$ or, equivalently, their vector representation $\mathbf{s}_m$. Their mean value is $\overline{\mathbf{s}} = \frac{1}{M}\sum_{m=1}^{M}\mathbf{s}_m$. Now, constructing a new set of

M signals by subtracting the mean from each of the $s_m(t)$ signals. Thus, $\mathbf{s}_m^{'} = \mathbf{s}_m - \overline{\mathbf{s}}$, with $m = 1, 2, \ldots, M$. The effect of this subtraction is the shift of the origin $s_m(t)$ signals to the origin.

The resulting signal constellation reveals the following properties:

- First, the energy per signal waveform is

$$\|\mathbf{s}_m^{'}\|^2 = \|\mathbf{s}_m - \overline{\mathbf{s}}\|^2 = E - \frac{2}{M}E + \frac{1}{M}E = E(1 - \frac{1}{M}) \tag{2.77}$$

- Second, the cross correlation of any pair of signals is

$$\frac{\mathbf{s}_m^{'} \cdot \mathbf{s}_n^{'}}{||\mathbf{s}_m^{'}||||\mathbf{s}_n^{'}||} = -\frac{1}{M-1} \tag{2.78}$$

  for all m, n.

Since only the constellation's centre of mass is translated, the distance between any pair of signal points is maintained at D, which is the same distance between any pair of orthogonal signals. For this reason, both P_e are equal.

The expressions 2.77 and 2.78 show that a set of simplex signals is equally correlated and require less energy, by a $1 - \frac{1}{M}$ factor when comparing with an orthogonal signal set. Hence, simplex signalling is employed when transmission's energy is limited.

These optimal properties define the so-called simplex signal set in a subspace with $N = M - 1$ dimensions, once the removal of the centre of mass lowers the number of dimensions by one. When M is large, there's little difference between the optimal simplex set and a set of equal-energy orthogonal signals because the factor $1 - \frac{1}{M}$ becomes closer to 1.

Simplex constellations reveal then some improvements comparing to orthogonal ones, losing only in the aspect that orthogonal signals are easier to generate and analyse than simplex signals [WJ65].

Chapter 3

Problem Formulation and Proposed Method

3.1 Mathematical Optimization

A mathematical optimization problem, or just optimization problem, has the form

$$\begin{aligned} &\text{minimize} \quad f_0(x) \\ &\text{subject to} \quad f_i(x) \leq b_i, \quad i = 1, ..., m \end{aligned} \tag{3.1}$$

Here, the vector $\boldsymbol{x} = (x_1, \ldots, x_n)$ is the optimization variable of the problem, the function $f_0 : \mathbf{R}^n \to \mathbf{R}$ is the objective function, the functions $f_i : \mathbf{R}^n \to \mathbf{R}\ , \quad i = 1, \ldots, m$ are the constraint functions, and the constants $b_1, \ldots, b_m$ are the limits for the constraints.
A vector $\mathbf{x}^\star$ is called optimal, or a solution of (3.1), if it has the smallest objective value among all vectors that satisfy the constraints. This is, for any z such as $f_1(z) \leq b_1, \ldots, f_m(z) \leq b_m$, we have $f_0(z) \geq f_0(x^\star)$.

3.1.1 Convex Optimization Problem

Optimization problems are divided by classes, characterized by particular forms of the objective and constraint functions. A convex optimization problem is one in which the

objective and constraint functions are convex, which means they satisfy the inequality

$$f_i(\alpha \boldsymbol{x} + \beta \boldsymbol{y}) \leq \alpha f_i(\boldsymbol{x}) + \beta f_i(\boldsymbol{y}) \tag{3.2}$$

for all $\boldsymbol{x}$, $\boldsymbol{y} \in R^n$ and all α, $\beta \in R$ with $\alpha + \beta = 1$, $\beta \geq 0$. Equivalently, a function is said to be convex if its epigraph (the set of points on or above the graph of the function) is a convex set. There is in general no analytical formula for the solution of convex optimization problems, but there are very effective methods for solving them [BV04].

3.1.2 Non-convex Optimization Problem

On the other hand, if the objective function and/or the constraint functions are not convex, it means that the optimization problem is categorized as a non-convex optimization problem. This kind of problems is known to be hard to solve, even for a small number of constraints. However, convex optimization also plays an important role in problems that are not convex. Combining convex optimization with a local optimization method it is possible to find an approximate, but convex, formulation of the problem for the original non-convex problem. Solving this approximate problem, it is obtained the exact solution to the approximate convex problem. This point may be used as the starting point for a local optimization method, applied to the original non-convex problem. Moreover, many methods for global optimization require a cheaply computable lower bound on the optimal value of the non-convex problem. The methods for doing this are based on convex optimization.

3.1.3 Non-convex QCQPs

A non-convex QCQP can be expressed in the form:

$$\begin{aligned} &\text{minimize } \ \boldsymbol{x}^T \boldsymbol{P}_0 \boldsymbol{x} + \boldsymbol{q}_0^T \boldsymbol{x} + r_0 \\ &\text{subject to } \ \boldsymbol{x}^T \boldsymbol{P}_i \boldsymbol{x} + \boldsymbol{q}_i^T \boldsymbol{x} + r_i \leq 0, \ i = 1, ..., m \end{aligned} \tag{3.3}$$

with variable $\boldsymbol{x} \in R^n$, and parameters $\boldsymbol{P}_i \in S^n$ (S^n represents the set of $n \times n$ matrices), $\boldsymbol{q}_i \in R^n$, and $r_i \in R$. In the case where all the matrices $\boldsymbol{P}_i$ are positive semidefinite, the

problem is convex and can be solved efficiently, otherwise the problem is a non-convex QCQP. This type of problems is *Non-deterministic Polynomial-time* (NP)-hard, which means that it is not straightforward to determine the complexity of the problem or respective solution time, by a polynomial. Globally they are difficult to solve, once its complexity grows exponentially with the problem dimensions.

This characteristic of non-convex QCQPs leads to the need of global optimization techniques. These techniques are based on convex optimization and are used to find a lower bound on the optimal value of the non-convex problem.

3.2 Problem Formulation

Following what was proposed to obtain, for a given pair *(N,M)* the goal is to find out the minimum energy constellation $\mathcal{C} = \{\boldsymbol{x}_1, \boldsymbol{x}_2, \ldots, \boldsymbol{x}_M\}$ with $\boldsymbol{x}_k \in \boldsymbol{R}^N$ for $k = 1, \ldots, M$, respecting yet the constraint that the Euclidean distance between different symbols (signals) must be greater or equal to a certain threshold.

This can be formulated as follows:

$$\mathcal{M} = \{(\boldsymbol{x}_1, \ldots, \boldsymbol{x}_M) : \|\boldsymbol{x}_i - \boldsymbol{x}_j\|^2 \geq D^2,\ 1 \leq i < j \leq M\} \tag{3.4}$$

where $\mathcal{M}$ is the M-sized vector of N-dimensional vectors [BD12].

Regarding this approach, it leads to the definition of the following merit function

$$f : \mathcal{M} \to \mathbb{R} \text{ and } \mathcal{C} = \{\boldsymbol{x}_1, \boldsymbol{x}_2, \ldots, \boldsymbol{x}_M\} \mapsto f(\mathcal{C})$$

as

$$f(\mathcal{C}) = \sum_{i=1}^{M} \|\boldsymbol{x}_i\|^2 \tag{3.5}$$

It is easily observed that $E_s = \frac{f(\mathcal{C})}{M}$, which means that this merit function $f(\mathcal{C})$ that was just defined is directly proportional to the symbol average energy, E_s.

Taking all this formulation to the next level: finding an optimum constellation $\mathcal{C} =$

$\{x_1, x_2, \ldots, x_M\}$ can be achieved by solving the optimization problem

$$\begin{aligned} \mathcal{C}^* &= \arg\min\ f(\mathcal{C}) \\ \mathcal{C} &\in \mathcal{M}\ , \end{aligned} \tag{3.6}$$

or equivalently

$$\text{minimize} \quad \sum_{i=1}^{M} \|\boldsymbol{x}_i\|^2 \tag{3.7}$$

$$\text{subject to} \quad \|\boldsymbol{x}_i - \boldsymbol{x}_j\|^2 \geq D^2. \tag{3.8}$$

Clearly, the objective function is $\sum_{i=1}^{M} \|\boldsymbol{x}_i\|^2$ with $x_i \in \mathbb{R}^N$ and its constraints are the inequalities $\|\boldsymbol{x}_i - \boldsymbol{x}_j\|^2 \geq D^2$, with $1 \leq i < j \leq M$.

The value of the threshold was chosen to be $D = 1$, once it doesn't affect the generality of the formulation given by (3.4).

The optimization problem is classified by the convexity of its constraints [BV04]. Since all the constraints in the set M are non-convex, this optimization problem is characterized as a non-convex optimization problem. Moreover, amongst the non-convex optimization problems class, this one is a non-convex Quadratically Constrained Quadratic Programming.

3.3 Proposed Method

The procedure now described is often called CCP. It is a simple technique but it will be proven to be an effective mean to achieve good compact multi-dimensional constellation designs that minimize the average symbols energy for a given minimum Euclidean distance. The software used to perform the algorithm is Matlab which has also the compatibility with the convex optimization tool CVX.

Following, there are the 4 steps figuring in the written algorithm.

- Encounter a feasible point $\boldsymbol{x}_0$
- Normalization of the constellation
- Linearization around $\boldsymbol{x}_0$

- CVX treatment of the SOCP

The linearization process and the calling of CVX are iterative. This means that steps 3 and 4 are executed recursively until the algorithm stops.

3.3.1 Encountering a feasible point

The first step is to randomly generate a $\mathcal{C}$ constellation such as $\mathcal{C} = \{\boldsymbol{x}_1, \boldsymbol{x}_2, \ldots, \boldsymbol{x}_M\}$, with $\boldsymbol{x}_k \in \mathbb{R}^N$ for $k = 1, \ldots, M$. This constellation has to be feasible facing the constraint (3.8), i.e., all the points of the constellation $\mathcal{C}$ must have the Euclidean distance between each pair of points equal or greater than one. If (3.8) cannot be respected, it is generated a new random set of N-dimensional points and the constraint is tested again. Once the constellation obeys to the constraint, the initial feasible point is found. It has dimension $[N \times M, 1]$ and it will be designed $\boldsymbol{x}_0$ from now on.
In figure 3.1 there is an example of an initial feasible point.

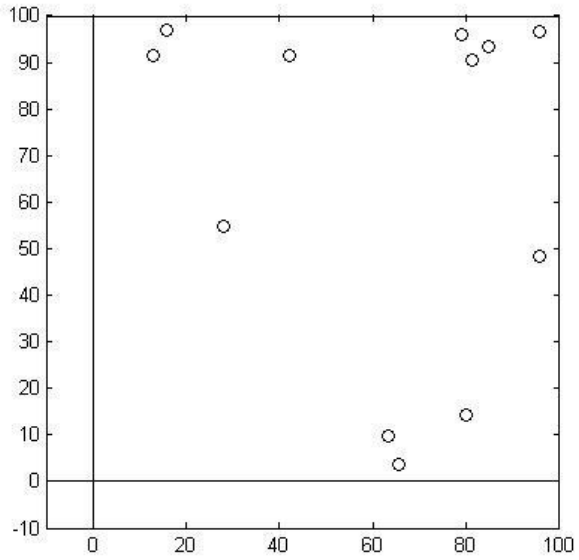

Figure 3.1: Feasible disposition for (N.M) = (2,12)

3.3.2 Normalization

Although a normalization process was optional, it was included in the method to allow the initial disposition of the constellation points to not be in the limit of the constraint. By this way it is given a certain freedom to the points to converge to the desired Euclidean distance.

Once the design of the optimum constellations is being done offline, the processing time is not a constraint.

What is done is simply normalize each vector $\boldsymbol{x}_i$, not with $D = 1$ but with a number a little bigger.

$$\boldsymbol{x}_i = \frac{\boldsymbol{x}_i}{\lambda.\sqrt{D}} \tag{3.9}$$

with $i = 1, \ldots, M$ and $\frac{1}{\lambda.\sqrt{D}}$ the normalization factor/value.

In the herein study, the normalization factor is $\lambda = 0.7$, turning the minimum distance between points to be $d_{min} \simeq 1.4286$ in the initial disposition.

The normalization of the feasible point of 3.1 by a $\lambda = 0.7$ factor is shown in figure 3.2.

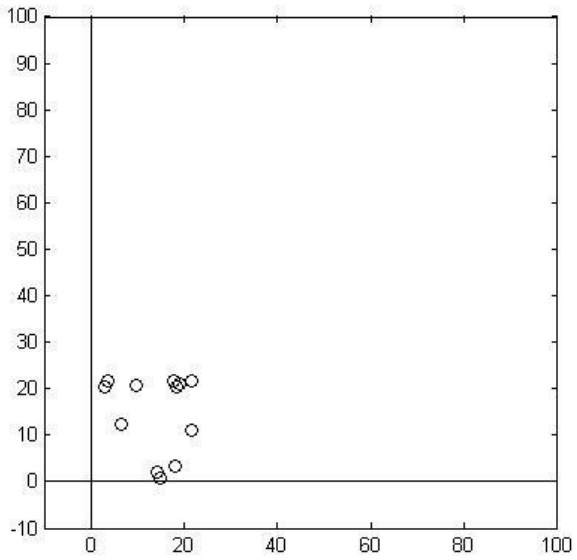

Figure 3.2: Normalized constelation by a $\lambda = 0.7$ factor
for (N.M) = (2,12)

3.3.3 Linearization

The next step consists of a reformulation of the non-convex constraints, i.e., 3.8 and successive linearization around the original feasible point $\boldsymbol{x}_0$ [dB03]. Here, the convex constraints shall be left unchanged, but once the formulated problem only possesses one

constraint and it is non-convex, it develops like follows:

$$\begin{aligned} \|\boldsymbol{x}_i - \boldsymbol{x}_j\|^2 &\geq 1 \\ (\boldsymbol{x}_i - \boldsymbol{x}_j)^T.(\boldsymbol{x}_i - \boldsymbol{x}_j) &\geq 1 \\ (\boldsymbol{x}_i^T - \boldsymbol{x}_j^T).(\boldsymbol{x}_i - \boldsymbol{x}_j) &\geq 1 \\ \boldsymbol{x}_i^T\boldsymbol{x}_i - \boldsymbol{x}_i^T\boldsymbol{x}_j - \boldsymbol{x}_j^T\boldsymbol{x}_i + \boldsymbol{x}_j^T\boldsymbol{x}_j &\geq 1\,, \quad 1 \leq i < j \leq M \end{aligned} \tag{3.10}$$

Here, $\boldsymbol{x}_i$ of size $[N, 1]$ similarly to $\boldsymbol{x}_j$, is defined by

$$\boldsymbol{x}_i = \mathbf{E}_i.\boldsymbol{x} \tag{3.11}$$

where $\mathbf{E}_i = \boldsymbol{e}_i^T \otimes \mathbf{I}_N$. $\boldsymbol{e}_i$ represents the i-th column of the identity matrix $\mathbf{I}_M$ and $\otimes$ denotes the Kronecker product.

To make it easier to understand, let's consider the case where $(N, M) = (2, 3)$.
Thus $\boldsymbol{x}$ will have the dimension $[N \times M, 1]$ and $\boldsymbol{x}_i$ dimension $[2, 1]$ and $\mathbf{E}_i$ will be $\boldsymbol{e}_i^T \otimes \mathbf{I}_N, \quad \forall\, 1 \leq i \leq M$.
After this, obtaining $\boldsymbol{x}_1$ comes: $\boldsymbol{x}_1 = \boldsymbol{E}_1.\boldsymbol{x}$ where $\mathbf{E}_1 = \boldsymbol{e}_1^T \otimes \mathbf{I}_2$

$$\mathbf{E}_1 \text{ comes } \begin{bmatrix} 1 & 0 & 0 \end{bmatrix} \otimes \begin{bmatrix} 1 & 0 \\ 0 & 1 \end{bmatrix} = \begin{bmatrix} 1 & 0 & 0 & 0 & 0 & 0 \\ 0 & 1 & 0 & 0 & 0 & 0 \end{bmatrix}$$

$$\text{and } \boldsymbol{x}_1 \text{ will be } \begin{bmatrix} 1 & 0 & 0 & 0 & 0 & 0 \\ 0 & 1 & 0 & 0 & 0 & 0 \end{bmatrix} . \begin{bmatrix} x_{11} \\ x_{21} \\ x_{31} \\ x_{41} \\ x_{51} \\ x_{61} \end{bmatrix} = \begin{bmatrix} x_{11} \\ x_{21} \end{bmatrix}$$

Respectively, $\boldsymbol{x}_2$ and $\boldsymbol{x}_3$ will be $\begin{bmatrix} x_{31} \\ x_{41} \end{bmatrix}$ and $\begin{bmatrix} x_{51} \\ x_{61} \end{bmatrix}$.

Replacing in (3.10), the values of $\boldsymbol{x}_i$ and $\boldsymbol{x}_j$ given by the expression (3.11), results

$$\begin{aligned} \mathbf{E}_i^T \boldsymbol{x}^T . \mathbf{E}_i \boldsymbol{x} - \mathbf{E}_i^T \boldsymbol{x}^T . \mathbf{E}_j \boldsymbol{x} - \mathbf{E}_j^T \boldsymbol{x}^T . \mathbf{E}_i \boldsymbol{x} + \mathbf{E}_j^T \boldsymbol{x}^T . \mathbf{E}_j \boldsymbol{x} \geq 1 \\ \boldsymbol{x}^T \left(\mathbf{E}_i^T \mathbf{E}_i - \mathbf{E}_i^T \mathbf{E}_j - \mathbf{E}_j^T \mathbf{E}_i + \mathbf{E}_j^T \mathbf{E}_j \right) \boldsymbol{x} \geq 1 \\ \boldsymbol{x}^T \left(\mathbf{E}_{ij} \right) \boldsymbol{x} \geq 1 \end{aligned} \tag{3.12}$$

where $\mathbf{E}_{ij}$ replaces the expression $\mathbf{E}_i^T \mathbf{E}_i - \mathbf{E}_i^T \mathbf{E}_j - \mathbf{E}_j^T \mathbf{E}_i + \mathbf{E}_j^T . \mathbf{E}_j \Leftrightarrow (\mathbf{E}_i - \mathbf{E}_j)^T . (\mathbf{E}_i - \mathbf{E}_j)$. It can be now verified

$$\begin{aligned} \| \boldsymbol{x}_i - \boldsymbol{x}_j \|^2 \geq 1 \Leftrightarrow \boldsymbol{x}^T \left(\mathbf{E}_{ij} \right) \boldsymbol{x} \geq 1 \Leftrightarrow \\ \Leftrightarrow 1 \leq \boldsymbol{x}^T \mathbf{E}_{ij} \boldsymbol{x} \end{aligned} \tag{3.13}$$

Thus, according to the document [dB03], where S. Boyd defines that the constraint of a general non-convex optimization problem of the format

$$\boldsymbol{x}^T \boldsymbol{P} \boldsymbol{x} + \boldsymbol{q}^T \boldsymbol{x} + r \leq 0 \tag{3.14}$$

can be rewritten as

$$\boldsymbol{x}^T \boldsymbol{P}_+ \boldsymbol{x} + \boldsymbol{q}_0^T \boldsymbol{x} + r_0 \leq \boldsymbol{x}^T \boldsymbol{P}_- \boldsymbol{x} \tag{3.15}$$

decomposing the matrix $\boldsymbol{P} \in \mathbf{S}^n$ into its positive and negative parts: $\boldsymbol{P} = \boldsymbol{P}_+ - \boldsymbol{P}_-$, with $\boldsymbol{P}_+,\ \boldsymbol{P}_- \succeq 0$.

Here, both sides of the inequality are convex quadratic functions, which means in advance that the non-convex QCQP problem was reformulated in order to be solvable.

Picking the constraint of inequality (3.16), it is noticeable that it is already on this format, where it verifies $\boldsymbol{P}_+ = 0$, $\boldsymbol{P}_- = \mathbf{E}_{ij}$, $\boldsymbol{q}^T = 0$ and $r = 1$. The right hand side of this equation

is then linearized around the feasible point $\boldsymbol{x}_0$, becoming the constraint of (3.2) of the form

$$\begin{aligned} 1 &\leq \boldsymbol{x}_0^T \mathbf{E}_{ij} \boldsymbol{x}_0 + 2\boldsymbol{x}_0^T \mathbf{E} ij \boldsymbol{x} - 2\boldsymbol{x}_0^T \mathbf{E}_{ij} \boldsymbol{x}_0 \\ 1 &\leq 2\boldsymbol{x}_0^T \mathbf{E} ij \boldsymbol{x} - \boldsymbol{x}_0^T \mathbf{E}_{ij} \boldsymbol{x}_0 \,, \quad 1 \leq i < j \leq M \end{aligned} \tag{3.16}$$

This linearization is only possible because $\mathbf{E}_{ij}$ is semidefinite positive, $\mathbf{E}_{ij} \succeq 0$, i.e., it is a Hermitian matrix with all eigenvalues non-negative. This can be proven by its definition on equation (3.12).

Done the linearization of the constraint around $\boldsymbol{x}_0$, the problem formulation set in (3.4) is now presented as

$$\mathcal{M}^\star = \{(\boldsymbol{x}_1, \ldots, \boldsymbol{x}_M) : 1 \leq 2\boldsymbol{x}_0^T \mathbf{E} ij \boldsymbol{x} - \boldsymbol{x}_0^T \mathbf{E}_{ij} \boldsymbol{x}_0,\ 1 \leq i < j \leq M\} \tag{3.17}$$

The right hand side of (3.16) is an affine lower bound of $1 \leq \boldsymbol{x}^T \mathbf{E}_{ij} \boldsymbol{x}$, changing the face of the problem: it turns the feasible set of the new formulation, a convex subset of the original feasible set, resulting the constraint to be convex instead of non-convex and thus more conservative.

A new feasible point $\boldsymbol{x}_1$ can now be achieved from the convex SOCP:

$$\begin{aligned} \text{minimize} \quad & \sum_{i=1}^{M} \|\boldsymbol{x}_i\|^2 \\ \text{subject to} \quad & 2\boldsymbol{x}_0^T \mathbf{E} ij \boldsymbol{x} - \boldsymbol{x}_0^T \mathbf{E}_{ij} \boldsymbol{x}_0 \geq 1 \,, \quad 1 \leq i < j \leq M \end{aligned} \tag{3.18}$$

3.3.4 CVX treatment of the SOCP

The convex SOCP result of the linearization, allows obtaining a new feasible point from (3.18) starting from a feasible point $\boldsymbol{x}_0$.

The use of the convex optimization software CVX, enters here, once it can solve efficiently this type of convex problems, returning a new feasible point $\boldsymbol{x}_1$ with a lower objective value.

If this process is repeated, after the problem is linearized around the output feasible points

that are returned by the program CVX, it is obtained a sequence of feasible points with decreasing objective values, this is, $\|\boldsymbol{x}_1\|^2 \leq \|\boldsymbol{x}_0\|^2$. However, the sequence doesn't go on indefinitely: the algorithm will stop when $\|\boldsymbol{x}_k - \boldsymbol{x}_{k+1}\| < 0.001$ for some k.
Remark that once the problem constraint is now convex, there is no need to keep checking if the output points belong to the feasible set of the problem: it is already implicit.
Finally, the constellation's centre of mass is shifted to the origin in order to minimize the average energy used to transmit each symbol.

3.4 Convex Optimization software - CVX

From the range of convex optimization programs and tools available to use in the project, CVX: Matlab Software for Disciplined Convex Programming, was preferred because a big part of the project's core was based on the book [BV04, "Convex Optimization"] from Stephen Boyd, the same author of the chosen software.
Briefly, CVX is a modeling system for constructing and solving *Disciplined Convex Programs* (DCP). It supports a number of standard problem types, including *Linear Programs* (LP) and *Quadratic Programs* (QP), SOCP, and *Semidefinite Programs* (SDP). It is also used to conveniently formulate and solve constrained norm minimization. CVX is implemented in Matlab, turning Matlab into an optimization modeling language. Model specifications are constructed using common Matlab operations and functions, and standard Matlab code can be freely mixed with these specifications.

3.4.1 Some used commands and notions

All CVX models must be preceded by the command *cvx_begin* and terminated with the command *cvx_end*. All variable declarations, objective functions, and constraints should fall in between.
All variables must be declared using the *variable* command. This command is composed by the name of the variable and an optional dimension list. For instance *variable X* declares a total of 326 (scalar) variables.
Declaring an objective function requires the use of *minimize* or *maximize* function, as appropriate. The objective function must be convex in minimization. Plus, one objective

function may be declared in a CVX specification at most and it must have a scalar value. Concerning to constraints, CVX supports comparison expressions like: Greater-than $\geq$, where the left-hand expression is concave, and the right-hand expression is convex.

Chapter 4

Numerical Results

In this chapter there will be presented the results of CCP method as well as their comparison with alternative modulations and/or results from other works considered good terms of comparison. These comparisons will verify the effectiveness of the proposed constellations.

There aren't many documents or even algebraic or geometrical studies referencing design of constellations, lattices, clusters, etc.. sharing the work objective, specially for dimensions greater than 4. It doesn't exist as well an analytic formula that features all pairs generated in terms of number of Euclidean dimensions and number of constellation points, hence these comparisons are essential to evaluate the performance of the produced constellations.

The present work varies its range of dimensions N from $2 \leq \mathrm{N} \leq 8$ and number of constellation points M where $M = 2^k$ with $k = 2, 3, \ldots, 8$, focusing on constellations of medium to small size.

4.1 Complexity of the method

Due to the complexity and consequent execution time of the method, the results were obtained offline and the best codes were stored. It was adopted a big number of trials in most of the cases, to obtain the best constellation's configuration.

In the context of this dissertation, time showed to be a serious constraint. Even though, for 4-point until 64-point constellation size, there were performed 100 trials. However, for

128-point constellations the algorithm was run 20 times and 10 for 256-point ones.

In an analytical approach, the procedure used to solve a SOCP convex problem, in the worst case, has complexity

$$\mathcal{O}\left(\left(\sqrt{1+\frac{M(M-1)}{2}}\right)\left((N+1)^2+2M(M-1\right)\right) \tag{4.1}$$

as it is described in [PT10].

The simulation times experienced and the equation (4.1) alert to the increased difficult obtaining results on constellations with a great number of symbols. For these reasons, the range of number of constellation points present in this work is $M = 2^k$ with $k = 2, 3, \ldots, 8$, focusing on constellations of small to medium size, mostly used in nowadays systems.

4.2 CCP constellations results

Constellations obtained are matrices like the following.

$$\begin{bmatrix}
3.1521 & 0.7201 & 3.5115 & 2.9642 & 3.2576 \\
3.1046 & 2.1211 & 0.8861 & 2.3279 & 1.5350 \\
2.2450 & 2.3160 & 2.1430 & 2.4791 & 1.9443 \\
1.3065 & 3.3698 & 2.8533 & 2.8798 & 1.6712 \\
1.8584 & 1.1869 & 1.0441 & 3.2848 & 0.7108 \\
0.9940 & 0.2464 & 0.5500 & 2.3157 & 2.0943 \\
1.8353 & 0.6699 & 1.2957 & 1.7506 & 0.2890 \\
0.5511 & 2.0323 & 3.1873 & 0.5761 & 0.7701 \\
3.4496 & 0.9650 & 1.1548 & 3.4021 & 0.7125 \\
1.9294 & 1.3329 & 0.3938 & 2.3162 & 1.7405 \\
2.3028 & 3.6553 & 3.3803 & 2.4817 & 2.8770 \\
0.3900 & 2.4404 & 0.6968 & 1.2918 & 1.2310 \\
0.3917 & 3.5592 & 3.6553 & 2.7171 & 2.3772 \\
2.1926 & 2.9379 & 0.0189 & 3.4764 & 3.3231 \\
3.2079 & 1.2532 & 3.7012 & 0.4667 & 2.5213 \\
1.6884 & 1.1273 & 3.4973 & 1.9939 & 0.5162
\end{bmatrix}$$

Figure 4.1: Constellation coordinates for N=5 and M=16

The best energy results of the new constellations are presented in figure 4.1 in order to proceed to a further comparison with equivalent schemes.

Energy values are represented in terms of *Asymptotic Code Gain* (ACG), once this parameter balances the ratio between constellation size and respective energy cost. For

(N,M) sets that aren't compared in the following sections, this value permits a reasonable interpretation of the constellation performance by itself.

ACG	N=2	N=3	N=4	N=5	N=6	N=7	N=8
M=4	1	1.33(3)	1.33(3)	1.33(3)	1.33(3)	1.33(3)	1.33(3)
M=8	0.6957	1.1344	1.5	1.5484	1.6364	1.7143	1.7143
M=16	0.4571	0.9170	1.2923	1.6	1.7010	1.8135	2
M=32	0.2817	0.6975	1.1031	1.4557	1.6928	1.8612	1.9709
M=64	0.1697	0.5213	0.8647	1.2418	1.5021	1.7678	2.0040
M=128	0.0989	0.3603	0.6911	1.0152	1.3906	1.5929	1.7918
M=256	0.0563	0.2562	0.5446	0.8498	1.1459	1.4221	1.6671

Table 4.1: Asymptotic Code Gain for CCP constellations

4.3 Performance results

This section will compare the performance of CCP constellations with benchmark schemes in use.

Remark that, in order to compare the new constellations with the existent ones, the latter ones had to be normalized with the purpose of fulfilling the minimum distance requirements: Euclidean distance between any two constellation symbols not smaller than 1.

4.3.1 Energy cost of 2-dimensional constellations

A considerable amount of literature exists on the problem of selecting an efficient set of N digital signals with in-phase and quadrature components for use in a suppressed carrier data transmission system.

The comparison with QAM, gradient descent and APSK 2-dimensional modulations is now presented, making the evaluation of the proposed method effectiveness easier.

4.3.1.1 CCP vs Gradient Descent

Foschini through a gradient-search algorithm proposed good constellations on which the asymptotic probability of error considering Gaussian noise is minimized under an average power constraint. His document [FGW74] presents some good 2-dimensional signal

constellations for M=4, M=7, M=8, M=16 and M=19 points, shown next:

- M=4

$$\mathcal{C} = \begin{bmatrix} I \\ Q \end{bmatrix} = \begin{bmatrix} 1.0 & 1.0 & -1.0 & -1.0 \\ 1.0 & -1.0 & 1.0 & -1.0 \end{bmatrix}$$

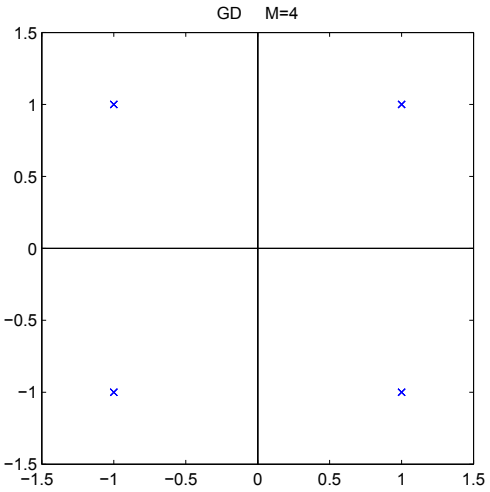

Figure 4.2: Gradient Descent constellation with M=4

- M=7

$$\mathcal{C} = \begin{bmatrix} I \\ Q \end{bmatrix} = \begin{bmatrix} 0.999 & -0.855 & -0.144 & 0.855 & 0.144 & 0 & -0.999 \\ -0.410 & -0.660 & 1.070 & 0.660 & -1.070 & 0 & 0.410 \end{bmatrix}$$

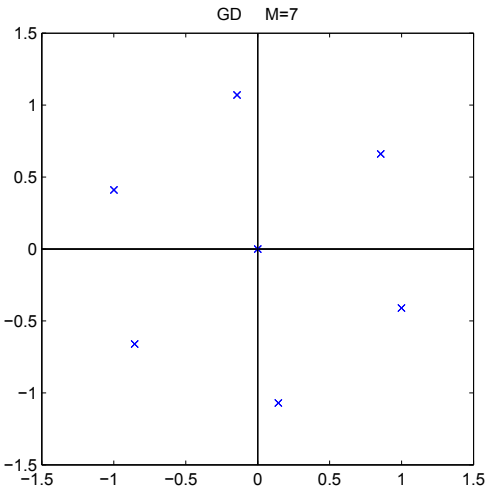

Figure 4.3: Gradient Descent constellation with M=7

- M=8

$$\mathcal{C} = \begin{bmatrix} I \\ Q \end{bmatrix} = \begin{bmatrix} 0.624 & -0.339 & 1.020 & -0.197 & -0.962 & 0.026 & -0.603 & 0.431 \\ 0.946 & 1.082 & 0.065 & -1.400 & 0.344 & 0.186 & -0.538 & -0.684 \end{bmatrix}$$

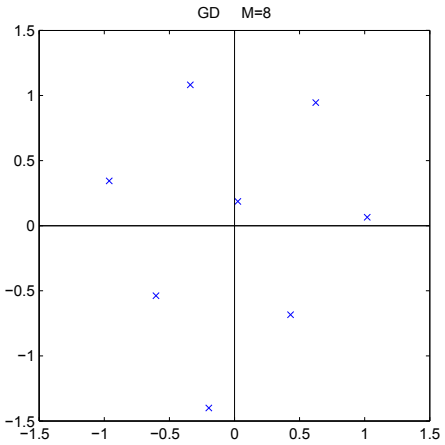

Figure 4.4: Gradient Descent constellation with M=8

- M=16

$$\mathcal{C} = \begin{bmatrix} I \\ Q \end{bmatrix} = \begin{bmatrix} 0.007 & 0.126 & 0.644 & 1.279 & 0.906 & -1.032 & -0.504 & -0.611 & 0.758 \\ 0.767 & 0.106 & 0.545 & 0.305 & -0.771 & -0.103 & 0.332 & 1.020 & -0.119 \end{bmatrix}$$

$$\begin{bmatrix} -0.911 & -0.388 & 0.245 & -0.272 & 0.376 & -1.136 & 0.512 \\ -0.772 & -0.329 & -0.552 & -1.001 & -1.215 & 0.571 & 1.211 \end{bmatrix}$$

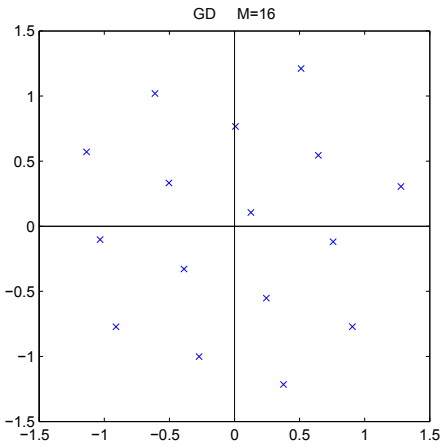

Figure 4.5: Gradient Descent constellation with M=16

- M=19

$$\mathcal{C} = \begin{bmatrix} I \\ Q \end{bmatrix} = \begin{bmatrix} 1.255 & -0.099 & 0.099 & -0.991 & -0.261 & 0.261 & 0.991 & -0.359 & 0.892 \\ -0.114 & -1.087 & 1.087 & -0.458 & 0.565 & -0.565 & 0.458 & -0.508 & -0.629 \end{bmatrix}$$

$$\begin{bmatrix} 0.359 & 0.726 & 0.529 & -0.892 & 0 & -1.255 & -0.529 & 0.620 & -0.620 & -0.726 \\ 0.509 & 1.030 & -1.144 & 0.629 & 0 & 0.114 & 1.144 & -0.056 & 0.056 & -1.030 \end{bmatrix}$$

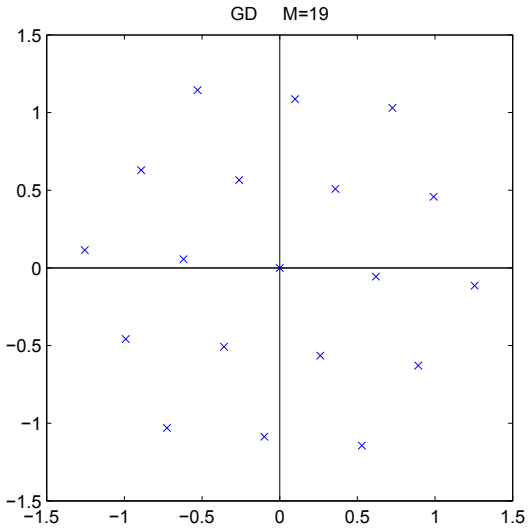

Figure 4.6: Gradient Descent constellation with M=19

The same group of 2-dimensional constellations was generated by the CCP method to be compared with the presented Gradient Descent modulations, evaluating the efficiency of CCP against this *Gradient Descent* (GD) method.

Next is presented the comparison of constellation energy costs and respective asymptotic code gains for both methods.

For M=4:

Convex-Concave Procedure			**Gradient Descent**	
Cost	ACG	**VS.**	Cost	ACG
2	1		2	1

Table 4.2: Comparison between CCP and GD for M=4

For M=7:

Convex-Concave Procedure			**Gradient Descent**	
Cost	ACG	**VS.**	Cost	ACG
6	0.8188		6.0025	0.8185

Table 4.3: Comparison between CCP and GD for M=7

For M=8:

Convex-Concave Procedure			**Gradient Descent**	
Cost	ACG	**VS.**	Cost	ACG
8.625	0.6957		8.8212	0.6802

Table 4.4: Comparison between CCP and GD for M=8

For M=16:

Convex-Concave Procedure			**Gradient Descent**	
Cost	ACG	**VS.**	Cost	ACG
35	0.4571		35.884	0.4459

Table 4.5: Comparison between CCP and GD for M=16

For M=19:

Convex-Concave Procedure			**Gradient Descent**	
Cost	ACG	**VS.**	Cost	ACG
48	0.4204		49.2025	0.4101

Table 4.6: Comparison between CCP and GD for M=19

As it can be noticed, the new constellations overperform the one produced by the GD method. For small sized constellations, the proposed ones are slightly better but that difference becomes greater with the increasing of the constellation size.

4.3.1.2 CCP vs APSK

In the document [DGGM06], Gaudenzi published good 4+12-APSK and 4+12+16-APSK constellations. These proposed signal constellations obey to a energy normalization $E[|x|^2] = 1$, which implies that the radii r_l of the APSK rings are normalized such as $\sum_{\ell=1}^{n_R} n_\ell r_\ell^2 = 1$, where the radii are ordered so that $r_1 < \ldots < r_\ell$.

Despite the shaping gains not being their strongest point, APSK signal constellations present good mutual information comparing to other conventional modulations.

Mutual information measures how much a random variable depends on another one. For a given signal set, it provides the maximum transmission rate at which error-free transmission is possible with such signal set. In other words, a great mutual information can be traduced in a significant reduction of the uncertainty over a random variable.

The document [DGGM06] states that for next generation broadband systems, the constellations sizes of interest are M=16 and M=32. Following this, it is proposed for a 16-ary constellation, a 4+12+16-APSK modulation with 2 rings and for the 32-ary constellation the respective 4+12+16-APSK constellation with 3 rings, both presented in the figure 4.7 and 4.8. Remark yet that the radii were not set arbitrarily: several ratios between the radius of the inner circle and the outer ones are presented in [DGGM06] and yet there were chosen for both modulations only the ones that achieved the lowest energy cost.

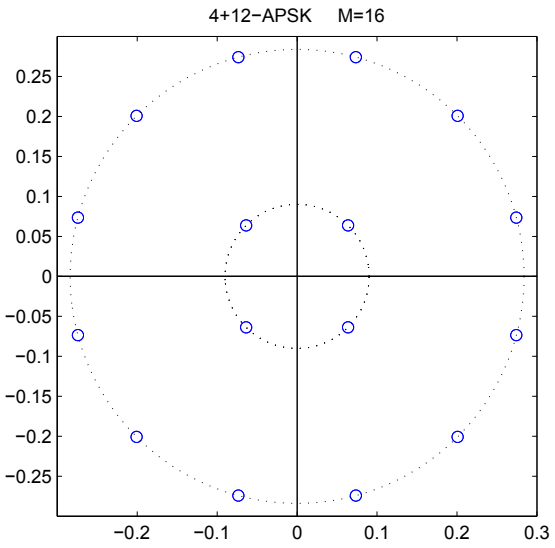

Figure 4.7: 4+12-APSK signal constellation
with $\rho = 2.70$, $r_1 = 0.09014$ and $r_2 = 0.283945$

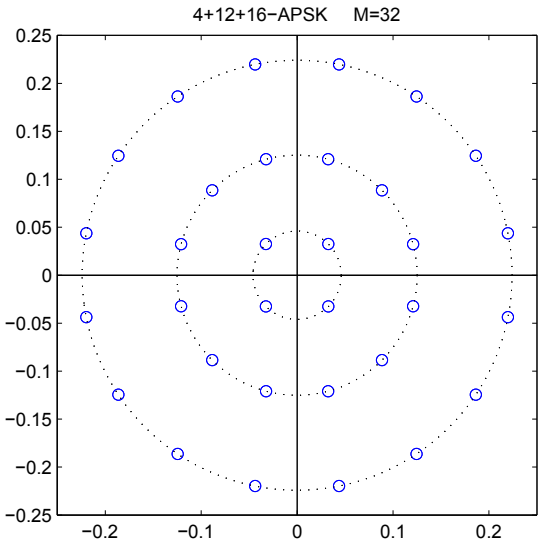

Figure 4.8: 4+12+16-APSK signal constellation with $\rho_1 = 2.53$, $\rho_2 = 4.3$, $r_1 = 0.046$, $r_2 = 0.125$ and $r_3 = 0.2241$

The energy cost and ACG of APSK constellations in comparison to CCP constellations, are shown in tables 4.7 and 4.8.

For M=16:

Convex-Concave Procedure			**4+12-APSK**	
Cost	ACG	**VS.**	Cost	ACG
35	0.4571		46.8323	0.3416

Table 4.7: Comparison between CCP and APSK for M=16

For M=32:

Convex-Concave Procedure			**4+12+16-APSK**	
Cost	ACG	**VS.**	Cost	ACG
140.0001	0.2817		219.6066	0.1821

Table 4.8: Comparison between CCP and APSK for M=32

From these comparisons, it is clear that the new proposed constellations offer much better power efficiency than the ones presented in [DGGM06].

4.3.1.3 CCP vs QAM

For the sake of a complete work, the comparison with QAM constellations performances is mandatory.

QAM constellations are known for having the best shaping gains amongst the 2-D constellations. This comes from the fact that it is possible to reduce the average symbol energy in a QAM constellation by using an approximately circular shape instead of a squared one.

The number of points in QAM constellations evolves by $(2n)^2$ where $\sqrt{number\,of\,points}$ is the number of bits in each constellation symbol[7]. Once there aren't any constellations with 7 or 8 symbols, the 7-QAM constellation and the 8-QAM constellations present in 4.9 are obtained from the standard 16-QAM constellation by removing the points with higher energy.

Similarly, both 19-QAM and 32-QAM constellations were obtained from the standard 36-QAM also removing the higher energy points as showed in figure 4.10.

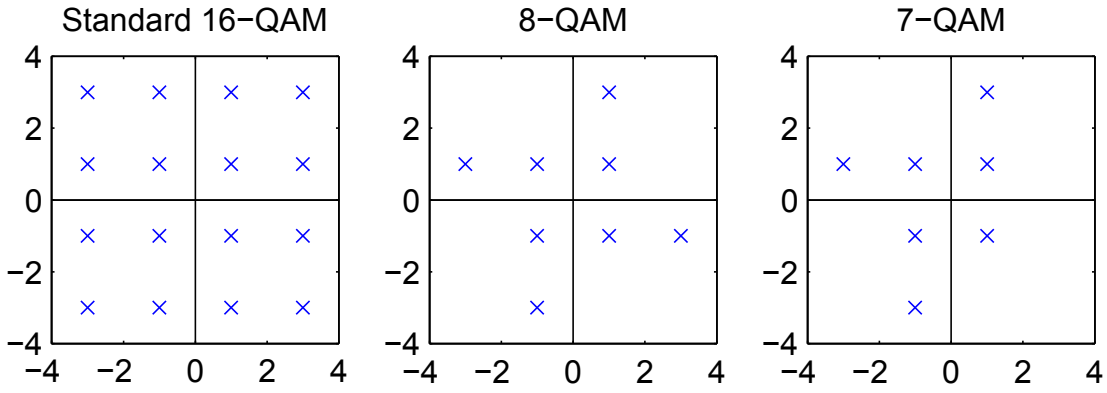

Figure 4.9: 16-QAM signal constellation and its derivatives
8-QAM and 7-QAM

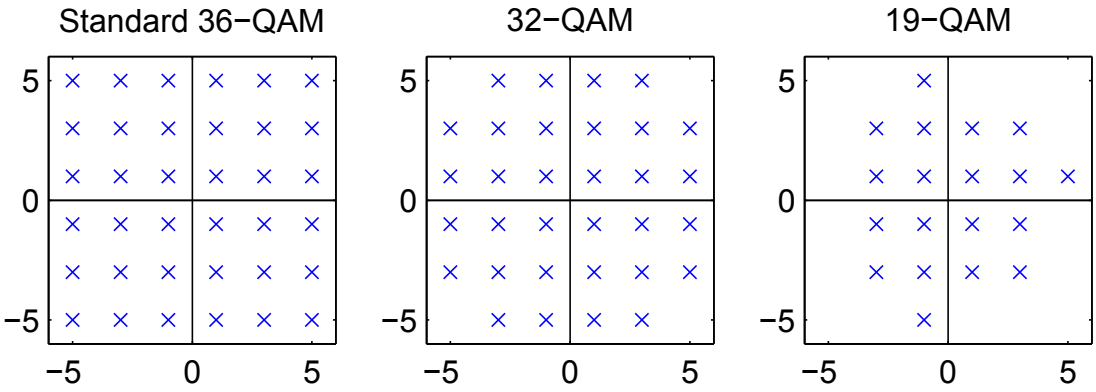

Figure 4.10: 36-QAM signal constellation and its derivatives
32-QAM and 19-QAM

The energy costs and respective ACG are presented on table 4.9.

	QAM		**Convex-Concave Procedure**	
Constellation size	**Cost**	**ACG**	**Cost**	**ACG**
4	2	1	2	1
7	9.5	0.5171	6	0.8188
8	12	0.5	8.625	0.6957
16	40	0.4	35	0.4571
19	59.5	0.3391	48	0.4204
32	160	0.25	142.0001	0.2817
36	210	0.2216	176.7500	0.2632

Table 4.9: CCP and QAM energy comparisons

As it can be seen, CCP values for same constellation sizes are better.

4.3.1.4 2-dimensions overall comparison

Finally, after gathering the values of the several modulations, the best way to interpret and judge the values is graphically.

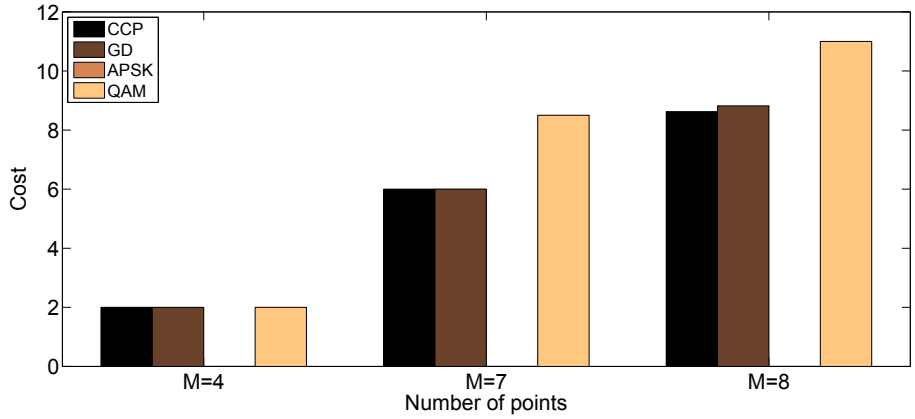

Figure 4.11: Comparison of CCP, GD, APSK and QAM for M=4, M=7 and M=8

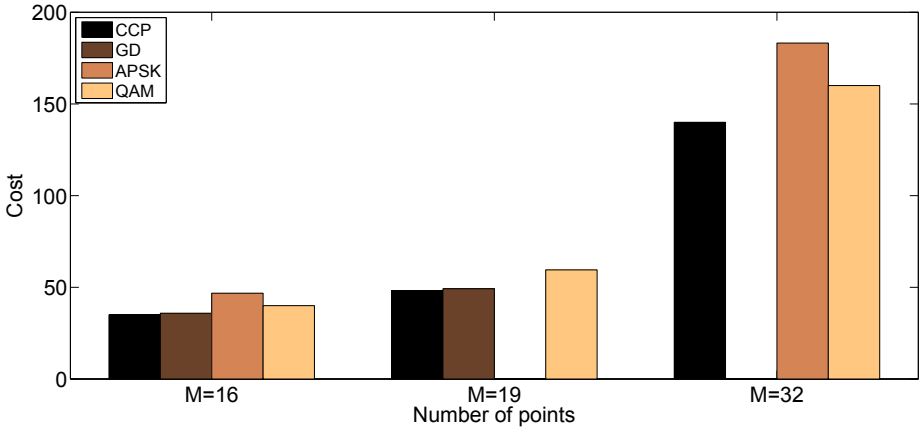

Figure 4.12: Comparison of CCP, GD, APSK and QAM for M=16, M=19 and M=32

Figures 4.11 and 4.12 show the energy cost of the different modulations for different constellation sizes. Note that the cost scale in y-axis is different on the 2 graphics what makes them to look alike.

In conclusion, it is possible to observe once more that the constellations obtained by the CCP method, show a better energy efficiency in all the cases comparing to the constellations revisited in [DGGM06] and [FGW74] and with standard QAM derivated ones.

4.3.2 Energies and gains for 3 and 4 dimension signal constellations

N. J. A. Sloane is an unavoidable name when dealing with minimal energy clusters. His work contains a really serious development in what concerns obtaining minimal energy clusters. More specifically, Sloane considers n equal nonoverlapping hard spheres and minimizes the second moment about the centroid [SHDC95] [Slo12]. Though it is a geometrical work, it is completely helpful in what concerns the design of good compact constellations. The reason is that, taking a closer look, having nonoverlapping spheres is equivalent to having points in Euclidean space keeping a minimal distance between them. Furthermore, minimizing the second moment about the centroid is proportional to reducing the energy of a multidimensional constellation and consequently to increase their ACG.

All this takes to the conclusion that Sloane's work is perfect for comparing with the proposed constellations for 3 and 4 dimensions. Denote, however, that [Slo12] contains results for (N,M)=(3,4) until (3,99) and for (N,M)=(4,4) until (4,32), which means that they only allow the comparison of some sets (N,M).

4.3.2.1 3-dimensional performance comparison

Table 4.10 shows Sloane's results for 3-dimensional clusters:

Dimension	**Nr Points**	**Moment**	**Energy**	**ACG**
3	4	6	1.5	1.3333
3	8	21.1566742	5.2892	1.1344
3	16	69.7925795	17.4481	0.9170
3	32	229.3750000	57.3438	0.6975
3	64	735.8333333	183.9583	0.5219

Table 4.10: 3-dimensional clusters' energy values

The CCP constellations attain exactly the same energy values of these 3-dimensional clusters.

4.3.2.2 4-dimensional performance comparison

Sloane's results for N=4 clusters are presented in table 4.11.

Dimension	Nr Points	Moment	Energy	ACG
4	4	6	1.5	1.3333
4	8	16	4	1.5
4	16	49.5232044	12.3808	1.2923
4	32	145.0449556	36.2612	1.1031

Table 4.11: 4-dimensional clusters' energy values

Similarly to the 3-dimensional results, the numbers of Sloane's work are the same as the ones obtained by the CCP method. This only highlights the importance of the proposed method that although it was not developed for 3 and 4 dimensional spaces it equals the very best results.

4.3.3 Orthogonal and related signal sets performance

Simplex signal sets are believed to be optimal for a given constellation size M when there is no constraint on dimension [VO79]. This comes from the fact that each signal can be represented in a different dimension from the other, minimizing interference between constellation symbols, which offers to CCP method a comparable signal set when N=M. The generated constellations matching this specification are (N,M)=(4,4) and (N,M)=(8,8) that denoted ACG 1.33 for the first pair and ACG=1.71 for the second.

Convex-Concave Procedure		**VS.**	**Simplex Constellations**	
Cost	ACG		Cost	ACG
1.5	1.33(3)		1.5	1.33(3)

Table 4.12: Comparison between CCP and simplex constellation for N=4 and M=4

Both sets, compared in table 4.12 and table 4.13, attain the same energy costs. This result places CCP constellations side by side with very good modulations in terms of *Intersymbol Interference* (ISI).

Convex-Concave Procedure		**VS.**	**Simplex Constellations**	
Cost	ACG		Cost	ACG
3.51	1.71		3.5	1.7143

Table 4.13: Comparison between CCP and simplex constellation for N=8 and M=8

Good signal constellations for schemes with $M = 2N$ are also known, as the case of bi-orthogonal constellations. Being an extension of regular orthogonal constellations, they allow the normal orthogonal constellation to have twice the number of signals.
The interest pairs of values that can bring up a comparison with the new constellations are $(N.M) = (4, 8)$ and $(N, M) = (8, 16)$ with ACG = 1.5 and ACG = 2 respectively.

Convex-Concave Procedure		**VS.**	**Bi-Orthogonal Constellations**	
Cost	ACG		Cost	ACG
4.0	1.5		4.0	1.5

Table 4.14: Comparison between CCP and Bi-Orthogonal Constellation for N=4 and M=8

Convex-Concave Procedure		**VS.**	**Bi-Orthogonal Constellations**	
Cost	ACG		Cost	ACG
8.0	2.0		8.0	2.0

Table 4.15: Comparison between CCP and Bi-Orthogonal constellation for N=8 and M=16

From tables 4.14 and 4.15, it can be seen that the CCP constellations have the same energy costs as these bi-orthogonal sets, as it can be verified in tables 4.14 and 4.15.

4.3.4 Multidimensional K-PAM constellations performance

The cartesian product of N identical K-PAM constellations originates a N-dimensional signal constellation with $M = K^N$ points [DXW11]. Although these PAM-based constellations are not characterized by great ACGs, they are, in this context, one valuable term

of comparison for higher dimension signal constellations obtained by the CCP method. The following $(K-PAM)^N$ constellations, can be compared to the range of the proposed constellations:

(N,M)	**Correspondent** $(K-PAM)^N$ **scheme**	**Energy Cost**	**ACG**
(3,8)	$(2-PAM)^3$	6	1
(4,16)	$(2-PAM)^4$	16	1
(5,32)	$(2-PAM)^5$	40	1
(6,64)	$(2-PAM)^6$	96	1
(7,128)	$(2-PAM)^7$	224	1
(8,256)	$(2-PAM)^8$	512	1
(3,64)	$(4-PAM)^3$	240	0.4
(4,256)	$(4-PAM)^4$	1280	0.4

Table 4.16: $(K-PAM)^N$ energy values

For every case represented on table 4.16, new constellations have better ACG values as it can be seen in table 4.17.

(N,M)	**Energy Cost**	**ACG**
(3,8)	5.2892	1.1344
(4,16)	12.3808	1.2923
(5,32)	27.4788	1.4557
(6,64)	63.9104	1.5021
(7,128)	140.6243	1.5929
(8,256)	307.1272	1.6671
(3,64)	187.7517	0.5113
(4,256)	940.1421	0.5436

Table 4.17: CCP energy values for $(K-PAM)^N$ possible sets

4.3.5 Kissing numbers

In general, constellations that attain the kissing number are considered to be good ones. The kissing number problem is a basic geometric problem that asks how many balls, of the same size, can touch one given ball simultaneously.

Talking in a $N = 2$ dimension approach, it reveals to be a very intuitive problem and can be formulated as: If you arrange pool balls on a pool table, how many balls can touch at the same time, the interior one. The answer is exactly 6 and it can be easily verified.

This simple answer leads to question: what if the number of involved dimensions increases? Contrarily to expected, this problem is far from easy and the sphere packing for N=3 also known as "Kepler conjecture" took many years to be solved. The concept of sphere packing problem can be intended as an extension of the 2-dimensional kissing number problem and it intends to determine the maximal density of a packing of spheres of the same size in Euclidean n-space.

Until recently, only exact solutions for $n = 1$, $n = 2$, $n = 3$, $n = 4$, $n = 8$ and $n = 24$ were known [PZ04]. The other dimensions haven't achieved yet a plausible conjecture for the best sphere packing. More, every dimension seems to have its own characteristics what makes the appearance of a pattern behaviour even more complicated.

It urged the necessity of confronting these solutions with the proposed method of compact constellations presented.

4.3.5.1 Comparison of kissing number constellations' values of energy vs CCP

- The best 2-D schemes are Voronoi constellations [CS83], that provide the densest configuration of the constellation's points over a hexagonal grid.

  The CCP algorithm was tested according to this optimal (N,M) set which has constellation energy 6. As it can be verified in the table 4.18, CCP returns as constellation energy value exactly 6.

- Regarding to 3-dimensions, with $(N, M) = (3, 13)$ the CCP signal constellation is compared with the lattice construction presented in [SC$^+$99] and as well with the values of energy in [PZ04]. It is verified that the lattice construction attains the kissing number with energy 12 through a icosahedron, represented with the lattice

H_3. Once again, CCP returns for the configuration $(N, M) = (3, 13)$ the value of energy 11.9253.

- In 4-dimensions and with $(N, M) = (4, 24)$, the lattice construction D_4 attains the kissing number with constellation energy of 24, exactly the same as through CCP.
- For 8-dimension it is known that lattice construction E_8 attains the kissing number with energy 240.
- Finally, regarding the 24-dimensions (by curiosity) the kissing number is attained with 196560, result supported by the lattice Λ_{24}. This value escapes greatly from the range of constellations studied in this work. Once, as it was explained before, the goal is to find out good compact signal constellations for small-to-medium size constellations and studying the method for constellation dimensions until N=8.

(N,M)	**Energy Cost**
(2,7)	6
(3,13)	11.9253
(4,24)	24

Table 4.18: Energy of kissing number schemes by CCP

4.4 Performance analysis

The new constellations are supposed to minimize the average energy per symbol. One way to achieve this is to compact the constellations symbols. Hence, symbols are already expected to have a greater number of neighbours than conventional constellations where symbols can be a little more spread.

In this work, two constellation symbols are considered neighbours if

$$1 \leq \|\boldsymbol{x}_i - \boldsymbol{x}_j\| \leq 1 + 0.05 \tag{4.2}$$

is verified. According to what was explained in subsection 2.1.3, the value of ϵ is 0.05. Set this parameter, the *Average Number of Nearest Neighbours* (ANNN), can be calculated

for each of the constellation sets and it is presented on the following table:

M \ N	**2**	**3**	**4**	**5**	**6**	**7**	**8**
4	2.5	3	3	3	3	3	3
8	3.5	4.5	6	6.25	6.75	7	7
16	4.125	5.625	7.75	10	11.1250	11.5	14
32	4.6875	7	9.6875	13.125	16.25	17.125	19.6250
64	5.0938	7.8750	9.1563	13.9688	15.2813	22.5313	27.0625
128	5.3438	7.2344	9.7656	12.7031	21.9062	19.9219	22.8594
256	5.5234	7.2734	10.3594	13.6719	16.9453	20.6328	24.6172

Table 4.19: ANNN for the generated constellations
with **N** - number of dimensions and **M** - number of symbols

As it can be seen, table 4.19 shows that the constellations obtained by the proposed method possess greater number of nearest neighbours per symbol when comparing to benchmark constellations of section 4.2 .

Although for minor SNR values a big ANNN value brings up some noise problems, with high SNR values its impact is smooth enough to not be a penalty. This can be confirmed comparing the *Symbol Error Rate* (SER), of the constellations generated with the ones referred before in 4.2 .

SER and error probability per symbol, P_s, in CCP constellations cannot follow a straight expression because the error probability always depends on the number of neighbours points around the transmitted symbol. Hence ANNN must be a multiplicative factor in the calculus on SER expression.

More, ANNN is an average indicator, which means that it doesn't return the exact number of neighbours for each symbol but the average number of neighbours per symbol instead. Regarding this, it is possible to present a very good approximated expression.

$$\text{SER} \approx \text{ANNN} \cdot Q\left(\sqrt{2 \cdot \text{ACG} \cdot \frac{E_b}{N_0}}\right) \tag{4.3}$$

Performance can be better judged on CCP constellations with higher number of symbols. It is extremely important to compare SER values with other modulations values. Hence, SER of the new constellations will be presented for cases $(N, M) = (4, 256)$, $(6, 64)$, $(7, 128)$ and $(8, 256)$ as well as for $(4 - \text{PAM})^4$, $(2 - \text{PAM})^6$, $(2 - \text{PAM})^7$ and $(2 - \text{PAM})^8$ cases of $(\text{K} - \text{PAM})^{\text{N}}$ constellations that can serve as a comparable scheme.

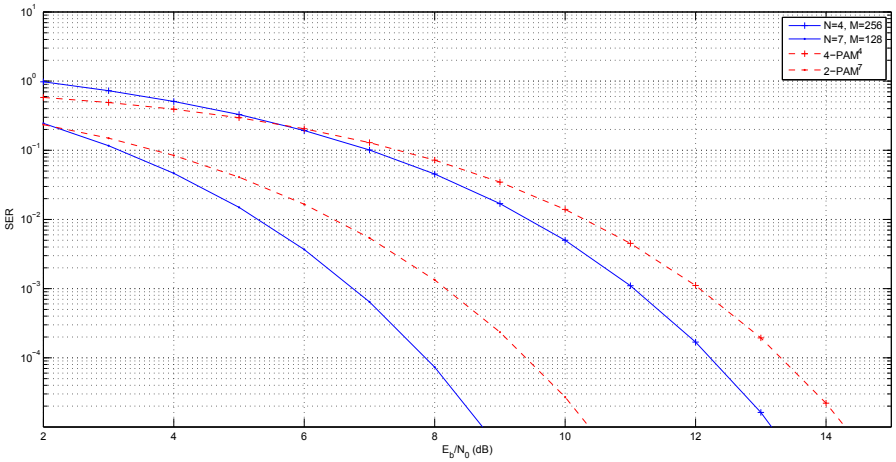

Figure 4.13: Performance comparison of CCP and $(\text{K} - \text{PAM})^{\text{N}}$ constellations for (N,M)=(4,256) and (7,128)

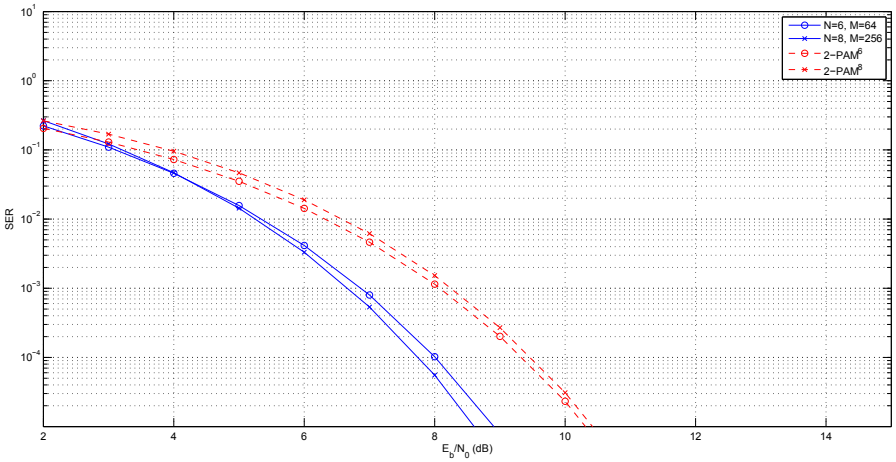

Figure 4.14: Performance comparison of CCP and $(\text{K} - \text{PAM})^{\text{N}}$ constellations for (N,M)=(6,64) and (8,256)

The interpretation of figures 4.13 and 4.14 shows clearly that the new constellations have a better performance than the equivalent schemes from $(\text{K} - \text{PAM})^{\text{N}}$ family.

All the generated constellations are compact, having each symbol a higher number of close

neighbours. They also have the centre of mass in the origin to eliminate the DC component and to minimize their energy cost.

Chapter 5

Conclusions

5.1 Final Considerations

This dissertation proposed a new view on designing good compact signal constellations that can minimize the average symbol energy respecting a minimum Euclidean distance between adjacent symbols. The design of the optimal constellations is formulated as a nonconvex optimization problem which is solved through an iterative process of linearization and treatment of a SOCP problem.

In chapter 2 the basics of signal spaces are presented and the detection theory is exposed. The definitions of signal energies, Euclidean distances, N-dimensional constellations are disclosed in a first stage. Follows the importance of the channel's noise and the design of the receiver mechanism that originates the estimation of the transmitted message. Finally, different modulations are described in terms of their performances, leading to the important ratio $\frac{D^2}{E_b}$.

Chapter 3 regards the formulation of the initial objective into a convex optimization scenario. It is established the objective function, the respective constraints and the merit function of the problem, which relates directly to the average symbol energy. The minimum distance to be respected between constellation symbols is defined here as well, turning clear the set of conditions under whose the work will be developed. Fitting the pattern of convex optimization, it is done the reformulation of the nonconvex QCQP problem into a SOCP problem which returns a new constellation with continuously lower objective values, satisfying the constraints at the same time.

The proof of the method's excellent results comes in chapter 4. The new constellations' comparison with the other modulations presented is very clear: they have better gains and respectively better power efficiency than QAM, GD and APSK constellations. The CCP constellations results showed along this chapter reveal that the proposed constellations overperform the ones used in present systems. Moreover, CCP constellations also show an increased number of ANNN for each point going in accordance with the definition of compact constellations.

5.2 Future Work

As future work, some suggestions and proposals can be done in the scope of using the potential and the substantial improvement that the new constellations offer comparing to the conventional ones:

- Usage of the good codes obtained in this work into the *hot topic* of optical and quantum wireless technologies [HHI+12];
- The combination of good multidimensional schemes with *Single-Carrier Frequency-Domain-Equalization* (SC-FDE) schemes in order to allow the definition of new efficient *Iterative Block Decision Feedback Equalisation* (IB-DFE) implementations suitable for multilevel constellations with low impact on system complexity [Ast12].

As a suggestion and once the algorithm wasn't run exhaustively for some of the biggest size constellations (like it was referred in section 4.1), it may be considered that little improvements are possible. Hence, the algorithm can be run longer, seeking for eventual enhancements.

Bibliography

[Ast12] Vítor Hugo Soares Astúcia. Linear amplification with multiple nonlinear devices. 2012.

[BD12] Marko Beko and Rui Dinis. Designing good multi-dimensional constellations. *Wireless Communications Letters, IEEE*, 1(3):221–224, 2012.

[BV04] Stephen Poythress Boyd and Lieven Vandenberghe. *Convex optimization*. Cambridge university press, 2004.

[CC75] A. Bruce Carlson and Paul B. Crilly. *Communication systems: an introduction to signals and noise in electrical communication*, volume 1221. McGraw-Hill New York, 1975.

[CS83] J. Conway and N. Sloane. A fast encoding method for lattice codes and quantizers. *Information Theory, IEEE Transactions on*, 29(6):820–824, 1983.

[dB03] Alexandre d'Aspremont and Stephen Boyd. Relaxations and randomized methods for nonconvex qcqps. *EE392o Class Notes, Stanford University*, 2003.

[DGGM06] Riccardo De Gaudenzi, A. Guillen, and Alfonso Martinez. Performance analysis of turbo-coded apsk modulations over nonlinear satellite channels. *Wireless Communications, IEEE Transactions on*, 5(9):2396–2407, 2006.

[DXW11] Ivan B. Djordjevic, Lei Xu, and Ting Wang. Coded multidimensional pulse amplitude modulation for ultra-high-speed optical transmission. In *Optical Fiber Communication Conference*. Optical Society of America, 2011.

[FGW74] G. Foschini, R. Gitlin, and S. Weinstein. Optimization of two-dimensional signal constellations in the presence of gaussian noise. *Communications, IEEE Transactions on*, 22(1):28–38, 1974.

[FHW98] Robert Fischer, Johannes Huber, and Udo Wachsmann. On the combination of multilevel coding and signal shaping. In *ITG Conf. Source and Channel Coding*. Citeseer, 1998.

[Hay88] Simon Haykins. *Digital communication*, volume 11. 1988.

[HHI+12] Lajos Hanzo, Harald Haas, Sándor Imre, Dominic O'Brien, Markus Rupp, and Laszlo Gyongyosi. Wireless myths, realities, and futures: from 3g/4g to optical and quantum wireless. *Proceedings of the IEEE*, 100(13):1853–1888, 2012.

[Pro01] John G. Proakis. Digital communications. 2001.

[PT10] Imre Pólik and Tamás Terlaky. Interior point methods for nonlinear optimization. In *Nonlinear Optimization*, pages 215–276. Springer, 2010.

[PZ04] Florian Pfender and Günter M. Ziegler. Kissing numbers, sphere packings, and some unexpected proofs. 2004.

[SC+99] Neil J. A. Sloane, John Conway, et al. *Sphere packings, lattices and groups*, volume 290. Springer, 1999.

[SHDC95] Neil J. A. Sloane, Ronald H. Hardin, T. D. S. Duff, and John H. Conway. Minimal-energy clusters of hard spheres. *Discrete & Computational Geometry*, 14(1):237–259, 1995.

[Slo12] Neil J. A. Sloane, http://neilsloane.com/cluster/index.html. Minimal-energy clusters, May 2012.

[VO79] Andrew J. Viterbi and Jim K. Omura. Principles of digital communication and coding, 1979.

[WJ65] John M. Wozencraft and Irwin Mark Jacobs. *Principles of communication engineering*, volume 1. Wiley New York, 1965.